

Short Title

Shell Matrix Proteins of *Nautilus pompilius*

Full Title

Hydrophilic Shell Matrix Proteins of *Nautilus pompilius* and The Identification of a Core Set of Conchiferan Domains

Authors

Davin H. E. Setiamarga^{1,2,3,*}, Kazuki Hirota^{1,10}, Masa-aki Yoshida⁴, Yusuke Takeda^{3,5}, Keiji Kito⁶, Keisuke Shimizu^{2,7}, Yukinobu Isowa^{2,8}, Kazuho Ikee⁹, Takenori Sasaki³, Kazuyoshi Endo²

Authors Affiliations

¹ Department of Applied Chemistry and Biochemistry, National Institute of Technology (KOSEN), Wakayama College, Gobo, Wakayama, Japan 644-0023

² Graduate School of Sciences, The University of Tokyo, Bunkyo, Tokyo, Japan 113-0033

³ The University Museum, The University of Tokyo, Tokyo, Japan 113-0033

⁴ Marine Biological Science Section, Education and Research Center for Biological Resources, Faculty of Life and Environmental Science, Shimane University, Oki, Shimane, Japan 685-0024

⁵ Graduate School of Science, Hokkaido University, Sapporo, Japan 060-0808

⁶ Department of Life Sciences, School of Agriculture, Meiji University, Kawasaki, Kanagawa, Japan 214-8571

⁷ Graduate School of Agriculture and Life Sciences, The University of Tokyo, Yayoi, Tokyo, Japan 113-8657

⁸ Shimoda Marine Research Center, University of Tsukuba, Shimoda, Shizuoka, Japan 411-8540

⁹ Center for Information Biology, National Institute of Genetics, Japan 411-8540

¹⁰ Present Address: Department of Biotechnology and Life Science, Tokyo University of Agriculture and Technology, Koganei, Tokyo, Japan 184-0012

* Corresponding author: dsetiamarga00@gmail.com, davin@wakayama.kosen-ac.jp

Keywords

biomineralization, proteomics, shell evolution, Mollusca, Cephalopoda

Abstract

Despite being a member of the shelled mollusks (Conchiferans), most members of extant cephalopods have lost their external biomineralized shells, except for the Nautiloids. Here, we report the result of our study to identify major Shell Matrix Proteins and their domains in the Nautiloid *Nautilus pompilius*, in order to gain a general insight into the evolution of Conchiferan Shell Matrix Proteins. In order to do so, we conducted transcriptomics of the mantle, and proteomics of the shell of *N. pompilius* simultaneously. Analyses of obtained data identified 61 distinct shell-specific sequences. Of the successfully annotated 27 sequences, protein domains were predicted in 19. Comparative analysis of *Nautilus* sequences with four Conchiferans for which Shell Matrix Protein data were available (the pacific oyster, the pearl oyster, the limpet, and the *Euhadra* snail) revealed that three proteins and six domains of the shell proteins are conserved in all Conchiferans. Interestingly, when the terrestrial *Euhadra* snail was excluded, another five proteins and six domains were found to be shared among the four marine Conchiferans. Phylogenetic analyses indicated that most of these proteins and domains were present in the ancestral Conchiferan, but employed in shell formation later and independently in most clades. Although further studies utilizing deeper sequencing techniques to obtain genome and full-length sequences, and functional analyses, must be done in the future, our results here provide important pieces of information for the elucidation of the evolution of Conchiferan shells at the molecular level.

Introduction

Many metazoans have evolved various biomineralized tissues, both internally and externally (Cowen, 2009). Despite its maintenance cost, many metazoan species have opted to retain the presence of such tissues because they are deemed useful, for example, for structural and morphological support, mineral ions storage, and protection and defense from predators and environmental factors (Lowenstam, 1989; Simkiss and Wilbur, 2012). Among extant metazoans, two phyla have anciently evolved and are still retaining their external biomineralized shells: the mollusks (Mollusca) and the brachiopods (Brachiopoda) (Cowen, 2009). Most members of these calcifying organisms live in the marine environment, where calcium and carbonate ions are easily available as sources of the mineralized tissues (Shimizu et al, 2019).

With ca. 85000 extant members, the phylum Mollusca is one of the most successful metazoan groups. Recent phylogenomics studies have shown that a monophyletic Mollusca is comprised of two groups, the non-shell forming Aculifera (Polyplacophorans and Aplacophorans) and the external shell-forming Conchifera, which is comprised of five families grouped further into two monophyletic clades: Monoplacophorans + Cephalopods clade and Scaphopods + Gastropods + Bivalves clade (Kocot et al., 2011; Smith et al., 2011; but see Kocot, 2013 and Kocot et al., 2020). Conchiferans' evolutionary success could probably be attributed to their ability to form mineralized external shells, which they might have acquired very early in their evolution during the Cambrian (Jackson et al., 2010; Shi et al., 2013).

The Conchiferan shell is arguably the most well studied external biomineralized structure (Marin et al., 2012). Mineralogy and microstructure studies have revealed that Conchiferan shells are mainly based on calcium carbonate, and composed of multiple calcified layers (such as the prismatic and nacreous layers) and one organic layer (the periostracum). The mechanism of shell formation is also similar among the Conchiferans: mantle tissue secretes various proteins related to mineral depositions, crystal formation breakage, pigmentation, etc. (Marin et al., 2012). Meanwhile, recent development of genomics, transcriptomics, proteomics, and other “-omics” approaches have allowed for detailed molecular characterizations of shell formation and biomineralization processes. Integration of

transcriptomics or Expressed Sequence Tag (EST) analysis with proteomics have revealed a list of genes involved in biomineralization processes in the mollusks (e.g. Zhang et al., 2012; Mann et al., 2012; Marie et al., 2012; Miyamoto et al., 2013; Zhao et al., 2018). Many of such proteins are present in trace amounts inside the shell, and thus called the Shell Matrix Proteins (SMPs). Despite their small amount, the SMPs have essential roles in shell formation and structural maintenance, such as calcium carbonate nucleation, crystal growth, and choice of calcium carbonate polymorphs (Addadi et al., 2006; Marin et al., 2008).

Among the five Conchiferan orders, the evolution of the cephalopods shell is arguably the most intriguing. While the group includes famous extinct members with univalve shells such as the ammonites and belemnites, almost all extant cephalopods internalized, reduced, or completely lost their shells (such as seen in some cuttlefishes, squids, and octopods). Only *Nautilus*, the last surviving genus of the basally diverging Nautilidae (\pm 416 MYA; i.e. Silurian/Devonian boundary) still have its external calcified true shells (Kröger et al., 2011). Another member of the cephalopods, the argonauts (Octopodiformes: Argonautidae) also have an external calcified shell. However, this shell is not a true shell because it lacks true shell microstructures, brittle, and most likely acquired secondarily from a shell-less Octopodiform ancestor, during the evolution of this group (Wolfe et al., 2012).

While much research on shell biomineralization genes, proteins, and protein domains have been done, most of these investigations are still biased towards bivalves and gastropods. This has hindered the elucidations of the origin and the evolution of the SMPs, including the prediction of the ancestral Conchiferan set of core protein domains needed for shell formation. Thus, in this study, we conducted transcriptomics of the mantle tissue and proteomics of the hydrophilic proteins extracted from the shell of the basal cephalopod *Nautilus pompilius* (Fig. 1). We used the transcriptome data of the mantle tissue as reference data to annotate the proteome data and thus to identify the protein sequences specifically located in the shell (the Shell Matrix Proteins; the SMPs). Comparative analyses were then conducted among the identified *Nautilus* SMPs and the publicly available representative Conchiferan SMP data of *Crassostrea gigas*, *Pinctada fucata*, *Lottia gigantea*, and *Euhadra quaesita*, in order to identify a conserved set of domains in

the Conchiferan SMPs. We also conducted a SEM electron microscopy analysis of the shell of *N. pompilius* to confirm that the shell morphology, at the microstructure level, is similar to the true shells of the Conchiferans.

Results

The microstructure of the shell of N. pompilius

Our Scanning Electron Microscopy (SEM) observation confirmed that the outer shell wall of *N. pompilius* is also composed of three layers of minerals, the outer and inner prismatic layers, and the nacreous layer in between (Fig. 2A; Grégoire, 1987; Marin et al., 2012). The outer prismatic layer is the outermost layer of the *Nautilus* shell wall and comprises ~25% of the total thickness of the adult shell wall. It consists of two sub-layers, the outer sub-layer composed of small crystallite grains and the inner sub-layer composed of prism-like elongate crystals whose long axis is oriented perpendicular to the shell surface (Fig. 2B). The nacreous layer, the middle layer of the *Nautilus* shell, is the thickest layer (~70%). It is composed of numerous thin plate-like tablets, whose thickness is less than 1 μm and oriented parallel to the inner shell surface. These tablets pile up one on top of another, forming columnar stacks (Fig. 2C). The inner prismatic layer comprises the innermost part of the shell. This layer is thin (~5%) and comprises prism-like elongate crystallites similar to those observed in the inner sub-layer of the outer layer (Fig. 2D).

Transcriptomics of the mantle tissue in N. pompilius

We conducted transcriptome sequencing using the ION-PGM platform of seven pieces (ca. 35 mg each) of the mantle tissue in seven separated runs, resulting in about five to six million reads per run (Table 1). After sequence assembly of all reads from the seven runs combined, 48,633 contigs were obtained, with the largest contig is 13,521 bp-long, the average length of contigs 414 bp, and the N50 value 419. Of these, 11,830 contigs (24.3%) encode ORFs longer than 100aa, which 8,092 encode proteins similar to those encoded in the draft genome of *O. bimaculoides*, and 3,738 encode non-registered polypeptides/proteins, which probably include novel (previously uncharacterized) protein sequences. Five of the most abundant transcripts in the mantle tissue showed no open reading frame (ORF). Five of the most abundant transcripts with ORF were shown in Table 2.

Sequence annotations and proteomics of Shell Matrix Proteins in *N. pompilius*

We conducted three runs of the LC-MS/MS mass spectrometer to analyze the extracted total proteins from the shell of a *Nautilus* individual for which the mantle transcriptomes were analyzed. A comparison between the obtained protein spectra from the MS/MS and the inferred protein spectra of the transcriptome contigs resulted in the identifications of 61 proteins. Of these, 14 contigs were not included in further analyses because they contain multiple translation frames, most likely frameshift error because of sequencing error.

Annotations of the remaining 47 contigs with single translation frames were conducted by doing BLASTp searches against three different databases: (1) the protein data of *Octopus bimaculoides* predicted from its genome (Albertin et al., 2015), (2) non-redundant (nr) Genbank sequence database, and (3) self-prepared database of known Shell Matrix Proteins (SMPs). The annotations were successful in identifying 27 sequences.

Homology comparisons of the Shell Matrix Proteins among several Conchiferan mollusks

We carried out reciprocal local BLASTn searches among the Shell Matrix Proteins (SMPs) of *N. pompilius* and selected five Conchiferans for which detailed SMPs data were available (as of July 2019: the pacific oyster *Crassostrea gigas*, the pearl oyster *Pinctada fucata*, the limpet *Lottia gigantea*, and the snail *Euhadra quaesita*), in order to identify conserved proteins and conserved protein domains among the SMPs in Conchifera. The searches were conducted with the threshold of $\geq 50\%$ sequence homology, and e-value of $\leq e^{-5}$ ("Search Setting 1"). Because of the stringency of our searches, and considering our highly fragmented transcriptome sequence data, there is a possibility that we did not pick up possibly conserved protein-coding gene sequences in our data. Therefore, we also conducted reciprocal local BLASTn searches using less stringent settings following previous studies (only by setting the maximum e-value of $\leq e^{-5}$; Shimizu et al., 2019; Zhao et al., 2018) ("Search Setting 2").

Reciprocal local BLASTx and tBLASTn searches of the 47 SMP sequences of the *Nautilus* as queries under Search Setting 1, found 43 proteins to be specific to

Nautilus (23 were annotated, while 20 were unknown proteins). However, the less stringent searches found 31 proteins (11 annotated, 20 unknown) to be specific to *Nautilus*. Meanwhile, searches using Search Setting 1 identified no protein, while Search Setting 2 identified additional three proteins (Pif/BMSP-like protein, CD109 antigen protein, and Tyrosinase) in all Conchiferans. Our most stringent searches identified another protein (EGF-ZP domain containing protein), and additional four (Chitinase, Peroxidase, Kunitz domain-containing protein, and *L. gigantea* LOTGIDRAFT_169029 (Chitin binding domain containing protein) by the less stringent searches, to be also shared among the four marine members, excluding *E. quaesita*. A complete list of the proteins is shown in Table 3. Meanwhile, results of the reciprocal local BLAST searches were shown as Circos charts, as shown in Fig. 3A and Supplementary Table 1 (for Search Setting 2), and Supplementary Fig. 1 and Supplementary Table 2 (for Search Setting 1).

Conserved domains of the Shell Matrix Proteins in Conchifera

Domain searches using Normal SMART (Letunic, 2018), PROSITE (Hulo et al., 2006), InterProScan (Jones et al., 2014), and NCBI (Altschul, 1990) databases predicted the presence of domain in 22 of the 27 annotated sequences. Meanwhile, of the unannotatable 20 contigs, domains were predicted in one contig. The diagrams showing the domains of the 22 + 1 sequences of *N. pompilius* are shown in Fig. 4A and listed in Supplementary Table 3. We manually searched for the presence of the identified domains in the other four Conchiferan Shell Matrix Protein (SMP) datasets. The result was summarized and shown in Fig. 4B, and Supplementary Tables 4–6. We found that six domains (A2M_comp, A2M_recep, Chitin-Binding Type 2 (ChtBD2), Signal peptide, Tyrosinase, and Von Willebrand factor type A (VWA)) were present in the five Conchiferans we analyzed in this study. When the terrestrial gastropod *E. quaesita* was excluded, additional six domains (An_peroxidase, Glyco_18 domain, Zona pellucida (ZP), Epidermal growth factor-like (EGF), BPTI/Kunitz family of serine protease inhibitors (KU), and Thiol-Ester bond-forming region (Thiol-ester_cl)) were found to be also shared among the four marine Conchiferans (Fig. 4B).

Phylogenetic analysis of the Shell Matrix Proteins in Conchifera

As mentioned previously, we identified a total of eight proteins (Pif/BMSP-like protein, CD109 antigen protein, Tyrosinase, Chitinase, Peroxidase, Kunitz domain-containing protein, *L. gigantea* LOTGIDRAFT_169029, and EGF-like domain containing protein) to be conserved among the four marine Conchiferans analyzed in this study. We conducted Maximum Likelihood phylogenetic inferences for the six successfully annotated proteins, in order to delve into their molecular evolutionary history. For the analyses, homologous metazoan protein sequences were mined from GenBank and UniProt, and included in the analyses. Phylogenetic analyses were conducted on the amino acid sequences of the proteins. The phylogenetic trees are shown in Fig. 5 (Pif/BMSP-like protein: Fig. 5A; CD109 antigen protein: Fig. 5B; Tyrosinase: Fig. 5C; Chitinase: Fig. 5D; Peroxidase: Fig. 5E; EGF-like domain containing protein: Fig. 5F)

Relatively robust phylogenetic trees were obtained for all six proteins, with most nodes supported moderately to strongly. Deeper nodes were unsupported, despite their general agreement with the accepted metazoan taxonomic classifications. The sequences form monophyletic groups at the phylum level (e.g. Mollusca), but not so at the lower taxonomic levels. All trees showed that the Shell Matrix Proteins (SMPs) are not monophyletic, and grouped together with non-SMP homologs in their consecutive phyla (Fig. 5).

Discussion

The shell of *N. pompilius* is a typical Conchiferan shell

Similar to other Conchiferans, the outer shells of Cephalopods are thought to also function by protecting their soft parts against predators. Shell morphological studies have indicated that outer shell breakages caused by fatal and nonfatal predatory attacks were often found in various extant *Nautilus* (e.g., Tanabe, 1988) and extinct, shelled cephalopod fossils (e.g., Takeda and Tanabe, 2015; Takeda et al., 2016). Moreover, members of Cephalopods had developed swimming ability, which had assisted their radiation both horizontally and vertically in the ocean habitat, in contrast to the rest of the marine Mollusks, which are mostly benthic. Among shelled Cephalopods, such swimming ability was acquired by the formation

of chambered shells (outer shell wall + internal septa), which functioned as a hydrostatic apparatus and unique to cephalopoda (e.g., Denton and Gilpin-Brown, 1966).

The microstructures of Conchiferan shell have been classified in several ways, based on their crystalized mineral morphology and architecture (Carter, 1990). The differing classification methods however agreed on the presence of the prismatic and nacreous layers, which have been observed in the shell of all Conchiferans including *N. pompilius*, various Bivalves (e.g. Pterioidea, Mytiloidea, and Nuculoidea) and Gastropods (e.g., Trochoidea and Haliotoidea). The wide occurrence of these types of microstructures among the Conchiferans strongly suggests that the *Nautilus* shell retains some of the ancestral characters of the Conchiferan shell, and thus most likely, its biomineralization processes. The similarities in shell microstructures and morphology of *Nautilus* and other Conchiferans, and some of their functions, thus underline the importance of dissecting the molecular underpinnings of the biomineralization of the *Nautilus* shell, in order to understand Conchiferan shell evolution, at the molecular, functional, and ecological levels.

Transcriptomics of the mantle tissue in N. pompilius using ION Torrent PGM is arguably enough to reveal the presence of several core Shell Matrix Proteins

In this study, we analyzed the transcriptome of several pieces of the mantle tissue obtained from three *N. pompilius* individuals. For the downstream analyses, we used a dataset built by combining all sequence reads from the seven pieces, and assembled them altogether. When analyzed together with the shell proteome data, we successfully identified 61 Shell Matrix Protein (SMP) sequences (47 SMPs = without frameshift errors), although not all of them were usable in further downstream analyses due to sequencing errors. However, the number of the obtained proteins is reasonable, when compared with other previous studies (e.g. *Euhadra quaesita* = 55, Shimizu et al., 2019; *Pinctada margaritifera* = 45, Marie et al., 2012; *Pinctada fucata* = 75, Liu et al., 2015; *Cepaea nemoralis* = 59, Mann and Jackson, 2014). One of the possible advantages of using a shallow system for transcriptome sequencing is that, most of the sequences we obtained here were

probably the most abundantly expressed transcripts, and thus, major SMPs, and not background expression genes accidentally picked-up. However, using a shallow next generation sequencing system such as ION-PGM also brings some disadvantages. For example, failure in domain predictions and annotations of several SMP contigs were probably because they were too fragmented and thus the sequences were incomplete, causing the annotation programs to be unable to detect any active domain sequences. There is also a possibility that sequencing errors might have caused mis-*in silico*-translations of some contigs. Of course, however, the possibility that some of the contained domains were unpredictable because they were novel domains, and that the 13 protein sequences are novel, previously uncharacterized proteins, cannot be eliminated by our present results.

For example, in this study, we were also unable to identify the only previously reported SMPs of the *Nautilus* thus far: Nautilin-63, which was extracted from the hydrophilic fraction of the shell of a congener of *N. pompilius*, *N. macromphalus* (Marie et al., 2011). This is probably caused by the shallowness of the sequencing system we presently employed. However, the possibility that this protein is species specific cannot be denied. Future analyses are still needed to see if Nautilin-63 is a major protein in all Nautiloids, or specific to *N. macromphalus*.

Therefore, in order to obtain the complete picture of SMPs in *N. pompilius*, further studies using deep transcriptome sequencing systems such as Illumina, and proteomics analyses of both the hydrophilic and hydrophobic component of the SMPs, are still needed in the future.

Homology comparisons and the evolution of the Shell Matrix Proteins among several Conchiferan mollusks

Homology searches among several Conchiferan mollusks for which the Shell Matrix Proteins (SMPs) have been studied as of July 2019 (the pacific oyster *Crassostrea gigas*, the pearl oyster *Pinctada fucata*, the limpet *Lottia gigantea*, and the snail *Euhadra quaesita*) revealed that three proteins (Pif/BMSP-like protein, CD109 antigen protein, and Tyrosinase; Fig. 3C) shared among the Conchiferans. The three proteins are known to be very important in maintaining shell structures. For example, the Pif/BMSP proteins are involved in the formation of the nacreous

layer of the shell, and thus crucial in forming and maintaining shell structure (Miyamoto et al., 2013; Suzuki et al., 2009; Suzuki et al., 2011). Pif and BMSP are composed of signal peptide, von Willebrand factor Type A domain (VWA), and Chitin-binding domains. VWA domain has function of the protein-protein interaction, Chitin-binding domain has the interaction with calcium ions in calcium carbonate (Suzuki et al., 2011). Meanwhile, Tyrosinase (both as a protein and a domain) is known to be involved in pigmentation (Nagai et al., 2007; Yao et al., 2020), and found in all mollusks compared in this study. Tyrosinase involvement in pigmentation is not only in the shell, but the protein was probably recruited and included inside the shell matrices to form the diverse coloration and patterns of the shell. In mammals including humans, the CD109 antigen protein is known to be involved in mineralized tissue formation, by being involved in osteoclast formations (Wang et al., 2013). Molecularly, it is a protease inhibitor, and it works by regulating TGF-beta receptor expression, TGF-beta signaling and STAT3 activation to inhibit TGF-beta signaling (Finsson et al., 2006; Litvinov et al., 2011).

Besides the three proteins detailed above, when the land snail *Euhadra quaesita* was excluded in the reciprocal BLASTx searches, another five proteins (EGF-ZP domain containing protein, Chitinase, Peroxidase, Kunitz domain-containing protein, and *L. gigantea* LOTGIDRAFT_169029 (Chitin binding domain containing protein) were found to be conserved among the marine Conchiferans (Fig. 3C). While it is very enticing to suggest that the difference in the types of proteins inside the shell matrices were caused by adaptation to the terrestrial environment, our analyses reported here cannot conclusively suggest so because of the differences in sequencing methods, sequencing depths, and completeness of the data compared. However, previous reports have suggested that the proteins reported as conserved among the marine Conchiferans were also probably important during shell formation. For example, the EGF-ZP domain-containing protein, Chitinase, and Peroxidase are suggested to be involved in the formation of calcium carbonate crystals in the shell (Iwamoto et al., 2020, Kintsu et al., 2017, Liao et al., 2019, Hohagen and Jackson, 2013). Future functional studies on these proteins, including the presently unknown *L. gigantea* LOTGIDRAFT_169029, must still be conducted in the future to investigate their specific functions during

Conchiferan shell formation.

Two proteins, Nucleobindin-like and Phospholipase A2-like proteins, were shown to be shared only between the limpet *L. gigantea* and *Nautilus*. Nucleobindin is known to be related to calcium ion binding in humans (Gaudet et al., 2011). Phospholipase A2 is a hydrolyzing enzyme which function of cleaving phospholipids depends on the presence of calcium ions (Dennis, 1994). While the specific function of both enzymes during shell formation and biomineralization has never been assessed, we could deduce that both enzymes are probably related to the calcification process of the shell. However, our analyses did not find these two enzymes in the shell matrices of other Conchiferans. This could be attributed not only to the exhaustiveness of data, but also to possible evolutionary scenarios, where the two genes were either lost by the other Conchiferan groups, or independently or recruited by *L. gigantea* and *Nautilus*. Interestingly, the traditional view of Molluscan taxonomy puts Gastropods as the sister group of Cephalopods (e.g. Yochelson et al., 1973, Salvini-Plawen and Steiner, 1996.). It is also to be noted that we found two Phospholipase A2-like proteins in *Nautilus*.

We did not find Nacrein-like protein in our *Nautilus* transcriptome and proteome data, although it is present in all other marine Conchiferans compared in this study. Interestingly, this protein is considered as one of the major soluble SMPs, and thus should be detected in our present data because we analyzed only the hydrophilic fraction of the *Nautilus* SMPs. However with our present data, we cannot say for certain that it is absent in the *Nautilus*. We believe that this protein should be present in all Conchiferans, although undetectable in our present *Nautilus* data. Future studies including the hydrophobic fraction of the SMPs of *Nautilus* using different sequencing platforms is still needed to clarify this issue.

Based on the information we presently obtained, we can deduce the Conchiferan core set of SMPs (Fig. 3C). However, phylogenetic analyses of the six proteins (Fig. 5A–F) showed that the SMPs were not monophyletic, as what would be expected if the proteins were specifically recruited once in the ancestral Conchiferan, to be used in shell formation. We found that the SMPs were not monophyletic even among closely related taxa/species. Therefore, with our present finding, we can deduce that the same proteins were probably recruited multiple

times in various taxa across Conchiferans, from preexisting proteins, which functions and structures were probably useful and easier to tinker for the formation of biomineralized structures.

Homology comparisons and the evolution of the Shell Matrix Proteins domains

From the 47 protein sequences we obtained from the shell of *N. pompilius*, we identified the presence of 19 domains (Fig. 4A). When compared with other the Shell Matrix Protein (SMP) data of the other Conchiferans analyzed in this study, we identified that five domains were conserved among all Conchiferans, and five additional domains were conserved among the marine species (Fig. 4B), and three domains were found only in *Nautilus*. They are common domains usually found in many proteins, including those unrelated to the biomineralization process in metazoans. However, we can deduce that the proteins containing the domains were recruited for shell formation, because the domains' known functions are most likely related to one or several activities/events during shell formation and maintenance, including the biomineralization process.

The Shell Matrix Proteins of N. pompilius

In this study, of the 47 proteins we successfully identified using both the transcriptome and proteome data, only 27 were successfully annotated. We were unable to annotate the 20 protein sequences, probably because they are too short, or previously uncharacterized novel protein sequences. However, the lack of sequence information thus prohibits us to deduce if the sequences were unique to *Nautilus*, or shared with other organisms we compared in this study.

Meanwhile, of the 27 sequences we annotated, we found 11 proteins (PFC0760c-like protein [*Octopus vulgaris*], Phospholipase A2-like [*Centruroides sculpturatus*], heme-binding protein 2-like [*Limulus polyphemus*], hypothetical protein KP79_PYT17609 [*Mizuhopecten yessoensis*], uncharacterized protein LOC110465975 [*Mizuhopecten yessoensis*], hypothetical protein KP79_PYT14004 [*Mizuhopecten yessoensis*], mucin-5AC-like isoform X2 [*Pomacea canaliculata*], uncharacterized protein LOC112572957 [*Pomacea canaliculata*], uncharacterized protein LOC112560033 isoform X3 [*Pomacea canaliculata*], and two Sushi-like

protein [*Mytilus coruscus*]) to be present only in the shell matrix of *N. pompilius* (Table 3). With only our present data, we are unable to actually say if the lack of these proteins in other Conchiferans biological or technical. For example, it is possible that the protein shared between *Nautilus* and the octopus (hypothetical protein OCBIM_22021924mg [*Octopus bimaculoides*]) are actually a protein sequence specific to the Cephalopods, while the heme-binding protein 2-like [*Limulus polyphemus*] are shared between Cephalopods and the Limulid Arthropods, the horseshoe crabs. Comprehensive future studies involving molecular evolution studies, comparative genomics, and functional analyses comparing these proteins are needed in order to obtain conclusive insights regarding their functions, and their specificity (or non-specificity) in the *Nautilus*.

It is also to be noted that we also found the EGF and ZP domains-containing protein in *N. pompilius* (Fig. 4A). The presence of the homologs of this protein in all Conchiferan SMPs including the basal cephalopod *Nautilus* might have underlined the importance of this protein during Conchiferan shell formation (Feng et al., 2017).

Acknowledgments

Declaration of conflict of interests. All authors declare that there was no conflict of interest at all, during the course of the study.

Ethical statement. All experiments were conducted in accordance to the guidelines and protocols of The University of Tokyo, in order to ensure proper and humane treatments of the experimental animals sacrificed during the course of this study.

Funding and research support. During the course of this study, DHES were initially supported by the JSPS Foreigner Postdoctoral Fellowship (F02330) with the entailing research grant awarded to KE (12F02330), and then partially by the FY2016 Research Grant for Chemistry and Life Sciences (The Asahi Glass Foundation), and the FY2017 Research Grant for Zoology (Fujiwara Natural History Research Foundation), both awarded to DHES. The study was also supported partially by the FY2018 Grant-in-Aid for Scientific Research (C) (Grant number: 18K06363) awarded to MAY (PI) and DHES (Co-PI). KE was partially supported by FY2011 Grant-in-Aid for Scientific Research (A) (Grant number: 23244101) and FY2011 Grant-in-Aid for

Challenging (Exploratory) Research (Grant number: 23654177). KS was supported by Grant-in-Aid for JSPS Fellows (Grant number: 12J09867).

DHES would like to thank the constant support and invaluable advice given by present and former members of the Setiamarga lab at NITW, former members of Endo lab at the University of Tokyo, and Takeshi Takeuchi (OIST).

Author contributions. DHES conceived the idea, initiated, and together with KE, managed the course of the study. DHES, HK, MAY, and KI conducted data analyses. DHES, TS, KS, and YT euthanized and dissected samples, which were then vouchered by TS at the museum. YT conducted shell microstructure analyses. DHES, HK, KS, YI, and KK conducted molecular works. DHES and HK wrote the first draft of the manuscript, which were then edited further by DHES, HK, MAY, YT, and KE. All authors confirmed the content of the final version of this manuscript.

Materials and Methods

Microstructure observations of the shell of *N. pompilius*

The microstructure of the outer shell of *N. pompilius* was examined by SEM (VE-8800, Keyence, Osaka, Japan). Samples of ~1 cm² were removed from the individual shell and their fracture surfaces were examined. Prior to the SEM observation, they were treated in etching with hydrochloric acid for 30 seconds. All samples were coated with platinum.

Sample collection and RNA extraction

We obtained three individuals of *N. pompilius* from a local dealer for aquarium shops in Japan. The samples were obtained from The Philippines. We obtained these samples at the end of 2011 and beginning of 2012, before the inclusion of this species in the CITES list and thus prior to the protected status of this species under the Washington agreement. First, we sedated the individuals in 2% ethanol in cold sea water for ca. 10 minutes (Butler-Struben et al., 2018). Afterward, we removed the shells of the individuals, and cut out pieces of the mantle tissue (ca. 25–35 mg each; Table 1) on ice, and stored them in ISOGEN (Nippon Gene Co. Ltd., Tokyo, Japan) at –80°C. Total RNA was extracted from the tissue samples using ISOGEN and the RNeasy kit (Qiagen), and was stored in –80°C until further transcriptome analyses. The rest of the body of the individuals were euthanized by freezing them in –80°C, and then preserved in formalin, to be later stored as vouchered specimens at The University Museum, The University of Tokyo, Japan.

Transcriptome analyses

Transcriptome sequencing of the mRNA extracted from the seven tissue samples, using the Ion Torrent PGM platform (Thermo Fisher Scientific) was outsourced to the Center for Omics and Bioinformatics, The University of Tokyo. Afterward, the obtained raw reads from the seven libraries made from the seven tissue samples were combined, and then assembled using the CLC assembly cell with the default settings on the Maser computing system, Data center for cell innovation, National Institute of Genetics (Kinjo et al. 2018). The Maser analytical pipelines on the National Institute of Genetics Cell Innovation program (

innovation. nigr.ac.jp/) were used for the following functional estimations of the assembled CLC contigs. For expression profiling, FASTQ reads were aligned to the CLC contigs using the TMAP mapping program (<https://github.com/iontorrent/TS/tree/master/Analysis/TMAP>). Raw read sequence data will be available in the DNA Data Bank of Japan (DDBJ).

Proteome analyses of total hydrophilic protein from the shell of N. pompilius

Shell of a *Nautilus* individual, for which the mantle transcriptomes were analyzed, was first shattered into pieces using a hammer. The shell pieces were cleaned from any organic tissue by incubation in a 2M NaOH overnight, and a thorough washing with Milli-Q water 10 times. Cleaned shell pieces were then ground into powder, and then slowly decalcified using 0.5 M EDTA as the chelating agent, at 4°C for 3 days. Total hydrophilic proteins of the shell were extracted using the 3 kDa Amicon Ultra Centrifugal Filter Unit.

After digestion into short peptides by trypsin (Promega), the samples were analyzed using a DiNa nanoLC system (KYA Technologies, Tokyo, Japan) and a LTQ Orbitrap mass spectrometer (Thermo Fisher Scientific). Identifications of obtained spectra were conducted by conducting a search on a self-prepared protein sequence database using the spectra as queries, using the SEQUEST program in Proteome Discoverer version 1.2 (Thermo Fisher Scientific). The self-made protein sequence database contained bioinformatically translated sequences of the assembled transcriptome contig data from the mantle tissue. These “theoretical” protein sequences were then fragmented into peptides *in silico* to simulate digestion by trypsin, in order to obtain the theoretical mass of peptides and MS/MS spectra. Spectrum data searches matched the actual experimental data of the actually obtained LC MS/MS spectra of the Shell Matrix Protein polypeptides, with the theoretical spectra database, resulting in the identification of candidate protein sequences from the database. Only transcriptome-based protein sequences matched by at least two LC MS/MS polypeptides were selected as potential Shell Matrix Proteins. Detailed methods and parameters for analyses were described in Elias and Gygi (2007), Isowa et al. (2015), and Shimizu et al. (2019).

Characterizations of the Shell Matrix Proteins of *N. pompilius*

Sequence annotation was performed by conducting BLASTp and BLASTx searches on the nr databases of Genbank and a database of published Conchiferan Shell Matrix Protein sequences, which we compiled ourselves by expanding the dataset of Arivalagan et al. (2017) and Feng et al. (2017).

Protein domains were predicted using multiple online tools: SMART (<http://smart.embl-heidelberg.de/>), PROSITE (<https://prosite.expasy.org/>), InterProScan (<https://www.ebi.ac.uk/interpro/search/sequence/>), and Pfam (HMMER v3.3; e-value <1.0e-5; <http://hmmer.org/>). Signal peptides were predicted using the online tool SignalP (Petersen et al. 2011). Predicted domains were visualized using an R script (Fig. 4A).

Comparative analysis of Conchiferan Shell Matrix Proteins

In order to identify conserved protein sequences among the five Conchiferan species analyzed in this study, the annotated 47 Shell Matrix Protein sequences of *N. pompilius* were used as queries in reciprocal local BLASTx and tBLASTn searches, against four molluscan for which the Shell Matrix Protein sequence data are already published (71 *Crassostrea gigas* proteins (Zhao et al, 2018); 159 *Pinctada fucata* proteins (Zhao et al 2018); 311 *Lottia gigantea* proteins (Mann et al 2012); 55 *Euhadra quaesita* proteins (Shimizu et al 2019)) (e-value <1e-5 and threshold $\geq 50\%$: “Search Setting 1”, e-value <1e-5: “Search Setting 2”). The result was visualized as Circos charts using the software Circos-0.69-9 (<http://circos.ca/>) (Fig. 3A).

The presence of homologous domains was confirmed manually, based on our reciprocal local BLAST result. The result was summarized and presented as a Venn diagram (Fig. 4B).

Phylogenetic analyses of the Shell Matrix Proteins

Phylogenetic analyses were conducted on a total of seven Shell Matrix Proteins obtained in this study (Tyrosinase, An-peroxidase, Chitinase, A2M receptor-domain containing Antigen-like protein, EGF-ZP, and BMSP). In order to do so, homologous amino acid sequences of each protein of various organisms

were data-mined from UNIPROT (<https://www.uniprot.org/>), including molluscan SMPs (if available / relevant), and non-SMPs. The presence of homologous domains in the sequences was confirmed using HMMER v3.1b2 (<http://hmmer.org>; e-values < 1.0e-5). These sequences were then aligned using the online version of MAFFT v7.310 (<http://mafft.cbrc.jp/alignment/server/index.html>; Katoh et al., 2002), with the g-INS-i algorithms to allow for global alignment (Katoh et al., 2005). Sequences were edited using the online version of GBlocks v.091b (Castresana, 2001) under the least stringent settings. Model selection was conducted on MEGA v10 (Tamura et al., 2011). Maximum Likelihood trees were inferred using the GUI version of RAxML (Silvestro et al 2012), with the rapid tree search setting and 1000 bootstrap replications, using the best fitting amino acid substitution model. The selected model for each protein is written directly in the figure showing the phylogenetic tree.

References

1. Addadi L., Joester D., Nudelman F., et al., 2006. Mollusk shell formation: a source of new concepts for understanding biomineralization processes. *Chemistry—A European Journal* 12, 980–987.
2. Albertin C., Simakov O., Mitros T., et al., 2015. The octopus genome and the evolution of cephalopod neural and morphological novelties. *Nature* 524, 220–224.
3. Altschul S. F., Gish W., Miller W., et al., 1990. Basic local alignment search tool. *Journal of Molecular Biology* 215, 403–410.
4. Arivalagan J., Yarra T., Marie B., et al., 2017. Insights from the shell proteome: biomineralization to adaptation. *Molecular Biology and Evolution* 34, 66–77.
5. Butler-Struben H. M., Brophy S. M., Johnson N. A., et al., 2018. *In vivo* recording of neural and behavioral correlates of anesthesia induction, reversal, and euthanasia in cephalopod molluscs. *Frontiers in Physiology* 9, 109.
6. Carter J.G., 1990. Skeletal biomineralization: patterns, processes and evolutionary trends. *Geol. Mag* 128, 411–413.
7. Castresana J., 2002. Genes on human chromosome 19 show extreme

- divergence from the mouse orthologs and a high GC content. *Nucleic Acids Research* 30, 1751–1756.
8. Cowen R. 2009. *History of Life (Fourth Edition)*. Massachusetts: Wiley-Blackwell.
 9. Dennis E.A., 1994. Diversity of group types, regulation, and function of phospholipase A2. *Journal of Biological Chemistry* 269, 13057–13060.
 10. Denton E.J., Gilpin-Brown J.B., 1966. On the buoyancy of the pearly *Nautilus*. *Journal of the Marine Biological Association of the United Kingdom* 46, 723–759.
 11. Elias J. E., Gygi S. P., 2007. Target-decoy search strategy for increased confidence in large-scale protein identifications by mass spectrometry. *Nature Methods* 4, 207–214.
 12. Feng D., Li Q., Yu H. et al., 2017. Identification of conserved proteins from diverse shell matrix proteome in *Crassostrea gigas*: characterization of genetic bases regulating shell formation. *Scientific Reports* 7, 45754.
 13. Finnson K. W., Tam B. Y., Liu K., et al., 2006. Identification of CD109 as part of the TGF- β receptor system in human keratinocytes. *The FASEB Journal* 20, 1525–1527.
 14. Gaudet P., Livstone M.S., Lewis S.E., et al., 2011. Phylogenetic-based propagation of functional annotations within the Gene Ontology consortium. *Briefings in Bioinformatics* 12, 449–462.
 15. Grégoire C., 1987. Ultrastructure of the Nautilus shell. In: Saunders WB, Landman NH. (Eds.), *Nautilus: The Biology and Paleobiology of a Living Fossil*, Plenum Press, New York, 463–486.
 16. Hohagen J., Jackson D. J., 2013. An ancient process in a modern mollusc: early development of the shell in *Lymnaea stagnalis*. *BMC Developmental Biology* 13, 1-14.
 17. Hulo N., Bairoch A., Bulliard V., et al., 2006. The PROSITE database. *Nucleic Acids Research* 34, D227-D230.
 18. Iwamoto S., Shimizu K., Negishi L., et al., 2020. Characterization of the chalky layer-derived EGF-like domain-containing protein (CgELC) in the pacific oyster, *Crassostrea gigas*. *Journal of Structural Biology* 212, 107594.

19. Jackson D.J., McDougall C., Woodcroft B., et al. Parallel evolution of nacre building gene sets in molluscs. *Molecular Biology and Evolution* 27, 591–608.
20. Jones P., Binns D., Chang H. Y., et al., 2014. InterProScan 5: genome-scale protein function classification. *Bioinformatics* 30, 1236–1240.
21. Katoh K., Misawa K., Kuma K. I., et al., 2002. MAFFT: a novel method for rapid multiple sequence alignment based on fast Fourier transform. *Nucleic Acids Research* 30, 3059–3066.
22. Katoh K., Kuma K. I., Toh H., et al., 2005. MAFFT version 5: improvement in accuracy of multiple sequence alignment. *Nucleic Acids Research* 33, 511–518.
23. Kinjo, S., Monma, N., Misu, S., et al. 2018. Maser: one-stop platform for NGS big data from analysis to visualization. *Database*, 2018.
24. Kintsu H., Okumura T., Negishi L., et al, 2017. Crystal defects induced by chitin and chitinolytic enzymes in the prismatic layer of *Pinctada fucata*. *Biochemical and Biophysical Research Communications* 489, 89–95.
25. Kocot K.M., 2013. Recent advances and unanswered questions in deep molluscan phylogenetics. *American Malacological Bulletin* 31, 195–208.
26. Kocot K. M., Cannon J. T., Todt C., et al., 2011. Phylogenomics reveals deep molluscan relationships. *Nature* 477, 452–456.
27. Kocot K. M., Poustka A. J., Stöger I., et al., 2020. New data from Monoplacophora and a carefully-curated dataset resolve molluscan relationships. *Scientific Reports* 10, 101.
28. Kröger B., Vinther J., Fuchs D., 2011. Cephalopod origin and evolution: A congruent picture emerging from fossils, development and molecules. *BioEssays* 33, 602–613.
29. Letunic I., Bork P., 2018. 20 years of the SMART protein domain annotation resource. *Nucleic Acids Research* 46, D493–D496.
30. Liao Z., Jiang Y. T., Sun Q., et al., 2019. Microstructure and in-depth proteomic analysis of *Perna viridis* shell. *PLoS One* 14, e0219699.
31. Litvinov I. V., Bizet A. A., Binamer Y., et al., 2011. CD109 release from the cell surface in human keratinocytes regulates TGF- β receptor expression, TGF- β signalling and STAT3 activation: relevance to psoriasis. *Experimental*

- Dermatology 20, 627–632.
32. Liu C., Li S., Kong J., et al., 2015. In-depth proteomic analysis of Shell Matrix Proteins of *Pinctada fucata*. Scientific Reports 5, 1–14.
 33. Lowenstam H.A.W.S., 1989. On biomineralization. New York: Oxford University Press.
 34. Mann K., Edsinger-Gonzales E., Mann M., 2012. In-depth proteomic analysis of a mollusc shell: acid-soluble and acid-insoluble matrix of the limpet *Lottia gigantea*. Proteome Science 10, 28.
 35. Mann K., Jackson D. J., 2014. Characterization of the pigmented shell-forming proteome of the common grove snail *Cepaea nemoralis*. BMC Genomics 15, 249.
 36. Marie B., Joubert C., Tayalé A., et al., 2012. Different secretory repertoires control the biomineralization processes of prism and nacre deposition of the pearl oyster shell. Proceedings of the National Academy of Sciences 109, 20986–20991.
 37. Marie B., Zanella-Cléon I., Corneillat M., et al., 2011. Nautilin-63, a novel acidic glycoprotein from the shell nacre of *Nautilus macromphalus*. The FEBS Journal 278, 2117–2130.
 38. Marie B., Jackson D. J., Ramos-Silva P., et al., 2012. The shell-forming proteome of *Lottia gigantea* reveals both deep conservations and lineage-specific novelties. FEBS Journal 280, 214–232.
 39. Marin F., Le Roy N., Marie B., 2012. The formation and mineralization of mollusk shell. Frontier in Bioscience 4, 1099–1125.
 40. Miyamoto H., Endo H., Hashimoto N., et al., 2013. The diversity of Shell Matrix Proteins: genome-wide investigation of the pearl oyster, *Pinctada fucata*. Zoological Science 30, 801–816.
 41. Nagai K., Yano M., Morimoto K., et al., 2007. Tyrosinase localization in mollusc shells. Comparative Biochemistry and Physiology Part B: Biochemistry and Molecular Biology 146, 207–214.
 42. Petersen T. N., Brunak S., Von Heijne, G., et al, 2011. SignalP 4.0: discriminating signal peptides from transmembrane regions. Nature methods, 8, 785–786.

43. Salvini-Plawen L., Steiner G., 1996. Synapomorphies and plesiomorphies in higher classification of Mollusca. Origin and evolutionary radiation of the Mollusca. Edited by: Taylor J.
44. Shi Y., Yu C., Gu Z., et al., 2013. Characterization of the pearl oyster (*Pinctada martensii*) mantle transcriptome unravels biomineralization genes. *Marine Biotechnology* 15, 175–187.
45. Shimizu K., Kimura K., Isowa Y., et al., 2019. Insights into the evolution of shells and love darts of land snails revealed from their matrix proteins. *Genome Biology and Evolution* 11, 380–397.
46. Silvestro D., Michalak I., 2012. raxmlGUI: a graphical front-end for RAxML. *Organisms Diversity and Evolution* 12, 335–337.
47. Simakov O., Marletaz F., Cho S.J., et al., 2013. Insights into bilaterian evolution from three spiralian genomes. *Nature* 493, 526–531.
48. Simkiss K, Wilbur KM., 2012. Biomineralization. New York: Elsevier.
49. Smith SA., Wilson NG., Goetz FE., et al., 2011. Resolving the evolutionary relationships of molluscs with phylogenomic tools. *Nature* 480, 364–367.
50. Somogyi E., Petersson U., Sugars R. V., et al., 2004. Nucleobindin—a Ca²⁺-Binding Protein Present in the Cells and Mineralized Tissues of the Tooth. *Calcified Tissue International* 74, 366–376.
51. Suzuki, M., Saruwatari, K., Kogure, T., et al., 2009. An acidic matrix protein, Pif, is a key macromolecule for nacre formation. *Science* 325, 1388–1390.
52. Suzuki M., Iwashima A., Tsutsui N., et al., 2011. Identification and characterisation of a calcium carbonate-binding protein, blue mussel shell protein (BMSP), from the nacreous layer. *Chembiochem* 12, 2478–2487.
53. Takeda Y., Tanabe K., 2015. Low durophagous predation on Toarcian (Early Jurassic) ammonoids in the northwestern Panthalassa shelf basin. *Acta Palaeontologica Polonica* 60, 781–794.
54. Takeda Y., Tanabe K., Sasaki T., et al., 2016. Durophagous predation on scaphitid ammonoids in the Late Cretaceous Western Interior Seaway of North America. *Lethaia* 49, 28–42.
55. Takeuchi T., Kawashima T., Koyanagi R., et al., 2011. Draft genome of the pearl oyster *Pinctada fucata*: a platform for understanding bivalve biology.

DNA Res 19, 117–130.

56. Tamura K., Stecher G., Peterson D., et al., 2013. MEGA6: molecular evolutionary genetics analysis version 6.0. *Molecular biology and evolution* 30, 2725–2729.
57. Tanabe K., 1988. Record of trapping experiment. Kagoshima University Research Center for the South Pacific, Occasional Papers 15, 5–15.
58. Wang Y., Inger M., Jiang H., et al., 2013. CD109 plays a role in osteoclastogenesis. *PloS One*, 8, e61213.
59. Wolfe K., Smith A. M., Trimby P., et al., 2012. Vulnerability of the Paper Nautilus (*Argonauta nodosa*) Shell to a Climate-Change Ocean: Potential for Extinction by Dissolution. *Biological Bulletin* 223, 236–244.
60. Yao H., Cui B., Li X., et al., 2020. Characteristics of a Novel Tyrosinase Gene Involved in the Formation of Shell Color in Hard Clam *Meretrix meretrix*. *Journal of Ocean University of China* 19, 183–190.
61. Yochelson E. L., Flower R. H., Webers G. F., 1973. The bearing of the new Late Cambrian monoplacophoran genus *Knightoconus* upon the origin of the Cephalopoda. *Lethaia* 6, 275–309.
62. Zhang G., Fang X., Guo X., et al., 2012. The oyster genome reveals stress adaptation and complexity of shell formation. *Nature* 490, 49–54.
63. Zhao R., Takeuchi T., Luo Y. J., et al., 2018. Dual gene repertoires for larval and adult shells reveal molecules essential for molluscan shell formation. *Molecular Biology and Evolution* 35, 2751–2761.

Figure Legends

Figure 1. (A) Phylogeny of Conchiferans including *N. pompilius*. (B) *N. pompilius*

Figure 2. The microstructures of *N. pompilius* shell.

(A) The shell microstructures of *N. pompilius*. (B) Outer prismatic layer. (C) Middle prismatic layer, (D) Inner prismatic layer.

Figure 3. Comparisons of the Shell Matrix Proteins in several Conchiferans for which the data are available using Search Settings 1. Detailed explanation of the settings is written in the main text. (A) Schematic presentation of the homologous relationships of the Shell Matrix Proteins among five Conchiferans (*Pinctada fucata*,

Crassostrea gigas, *Lottia gigantea*, and *Euhadra quaesita*). (B) Venn diagram showing the numbers of shared proteins identified through local BLASTp searches among the five Conchiferans. (C) Homologous proteins of the five Conchiferans compared, plotted on to the phylogeny of the animals.

Figure 4. Comparisons of the domains contained in the Shell Matrix Proteins of several Conchiferans for which the data are available. (A) Schematic representations of the domains in the Shell Matrix Proteins of *N. pompilius*. (B) Shared domains in the Shell Matrix Proteins of the five Conchiferans (*Pinctada fucata*, *Crassostrea gigas*, *Lottia gigantea*, and *Euhadra quaesita*) compared, plotted on to the phylogeny of the animals. The reconstructed Ancestral Conchiferans most likely had all of the shared domains.

Figure 5. Phylogenetic trees of selected Shell Matrix Proteins.

(A) The maximum likelihood tree of the Pif/BMSP amino acid sequences, inferred using the LG + Γ model with 1000 bootstrap replicates. (B) The maximum likelihood phylogenetic tree of A2M related CD109 antigen Protein, inferred using the LG + Γ model with 1000 bootstrap replicates. (C) The maximum likelihood phylogenetic tree of Tyrosinase inferred under the LG + Γ + I model with 1000 bootstrap replicates. (D) The maximum likelihood phylogenetic tree of Chitinase inferred under the LG + Γ

model with 1000 bootstrap replicates. (E) The maximum likelihood tree inferred from Tyrosinase amino acid sequences under the LG + Γ model with 1000 bootstrap replicates. (D) The phylogenetic tree inferred from Peroxidase amino acid sequences under the LG + Γ model with 1000 bootstrap replicates. (F) The phylogenetic tree of the EGF-ZP Protein under the WAG + Γ model with 1000 bootstrap replicates. Bootstraps values <30% are not shown, and a black square on a node indicate 100% bootstrap support.

Abbreviations: Pifu: *Pinctada fucata*, Crgi: *Crassostrea gigas*, Apca: *Aplysia californica*, Bigl: *Biomphalaria glabrata*, Logi: *Lottia gigantea*, Miye: *Mizuhopecten yessoensis*, Miga: *Mytilus galloprovincialis*, Phau: *Phoronis australis*, Euqu: *Euhadra quaesita*, Drfi: *Drosophila ficusphila*, Trps: *Trichinella pseudospiralis*, Hosa: *Homo sapiens*, Lili: *Littorina littorea*, Mumu: *Mus musculus*, Pimar: *Pinctada margaritifera*, Pimax: *Pinctada maxima*, Ptpe: *Pteria penguin*, Hala: *Haliotis laevigata*, Ilar: *Illex argentine*, Seof: *Sepia officinalis*, Cael: *Caenorhabditis elegans*, Drme: *Drosophila melanogaster*, Pale: *Pacifastacus leniusculus*, Bomo: *Bombyx mori*, Gaga: *Gallus gallus*, Hadi: *Haliotis discus*, Myco: *Mytilus coruscus*, Mytr: *Mytilus trossulus*, Ocvu: *Octopus vulgaris*, Toca: *Toxocara canis*, Pimarg: *Pinctada margaritifera*, Rano: *Rattus norvegicus*.

Contig denotes the *N. pompilius* sequence obtained in this study.

Supplementary Figure Legends

Supplementary Figure 1. Comparisons of the Shell Matrix Proteins in several Conchiferans for which the data are available using Search Settings 2. Detailed explanation of the settings is written in the main text.

Fig. 1

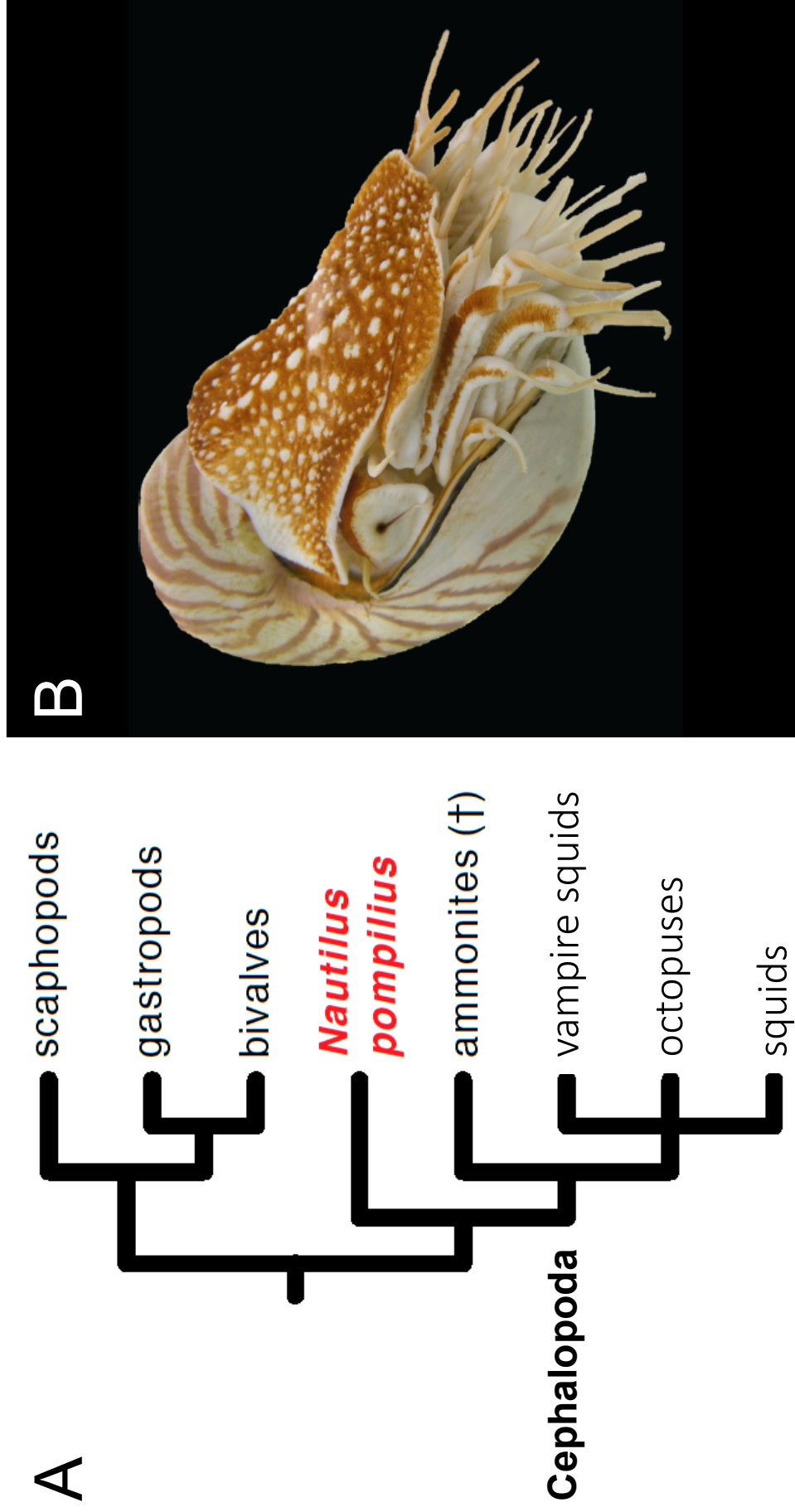


Fig. 2

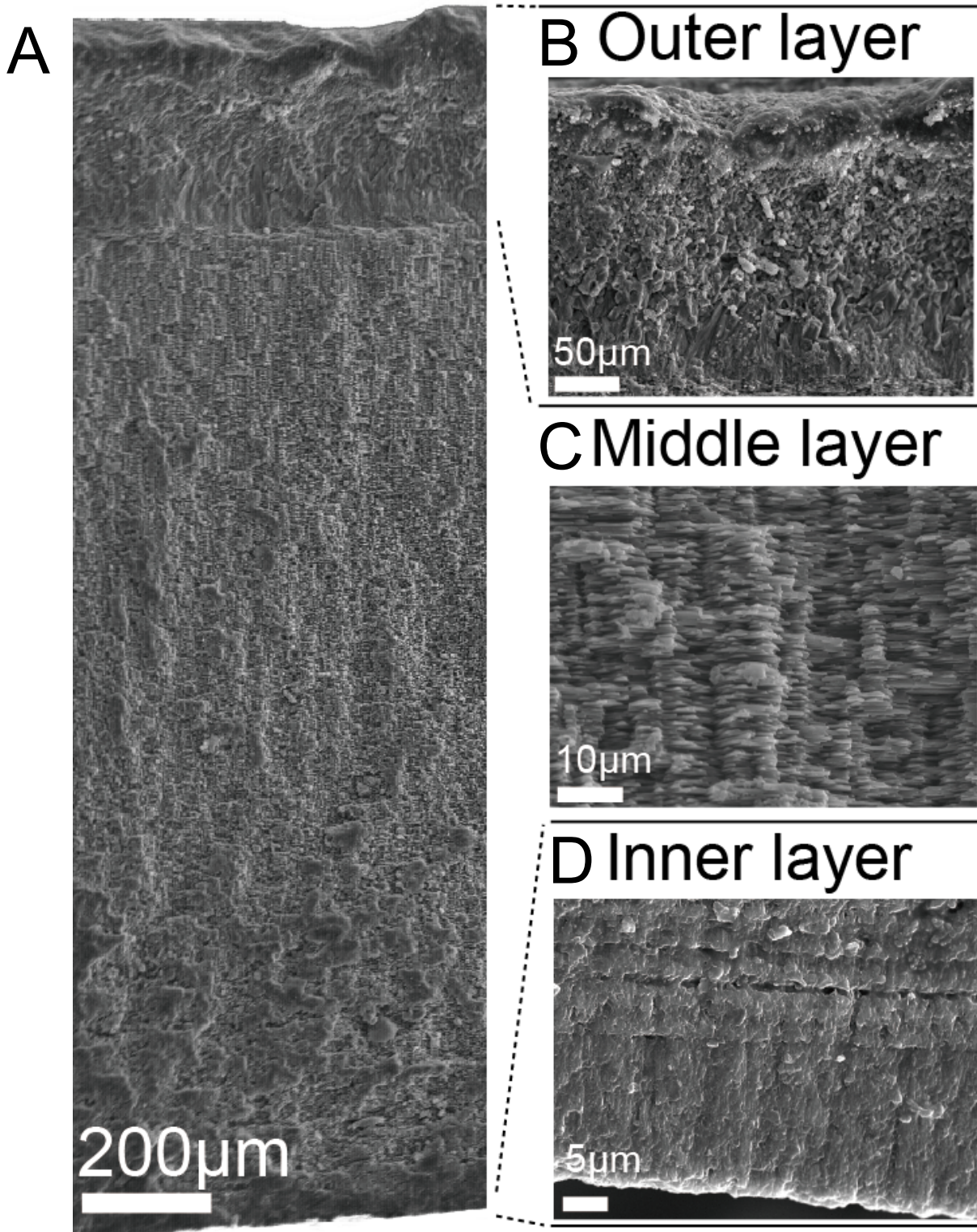


Fig. 3

A

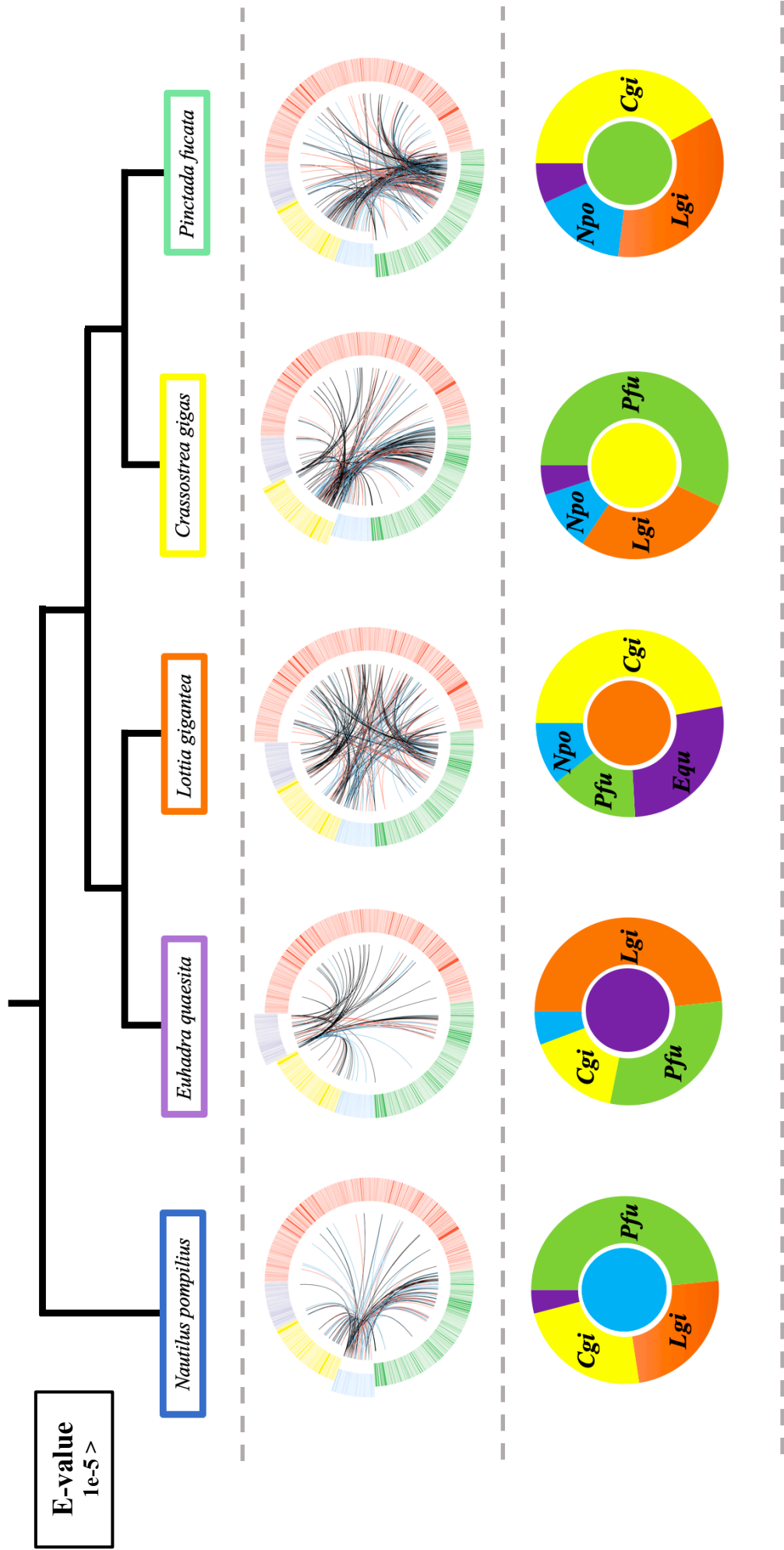


Fig. 3

B

E-value
 $1e-5 >$

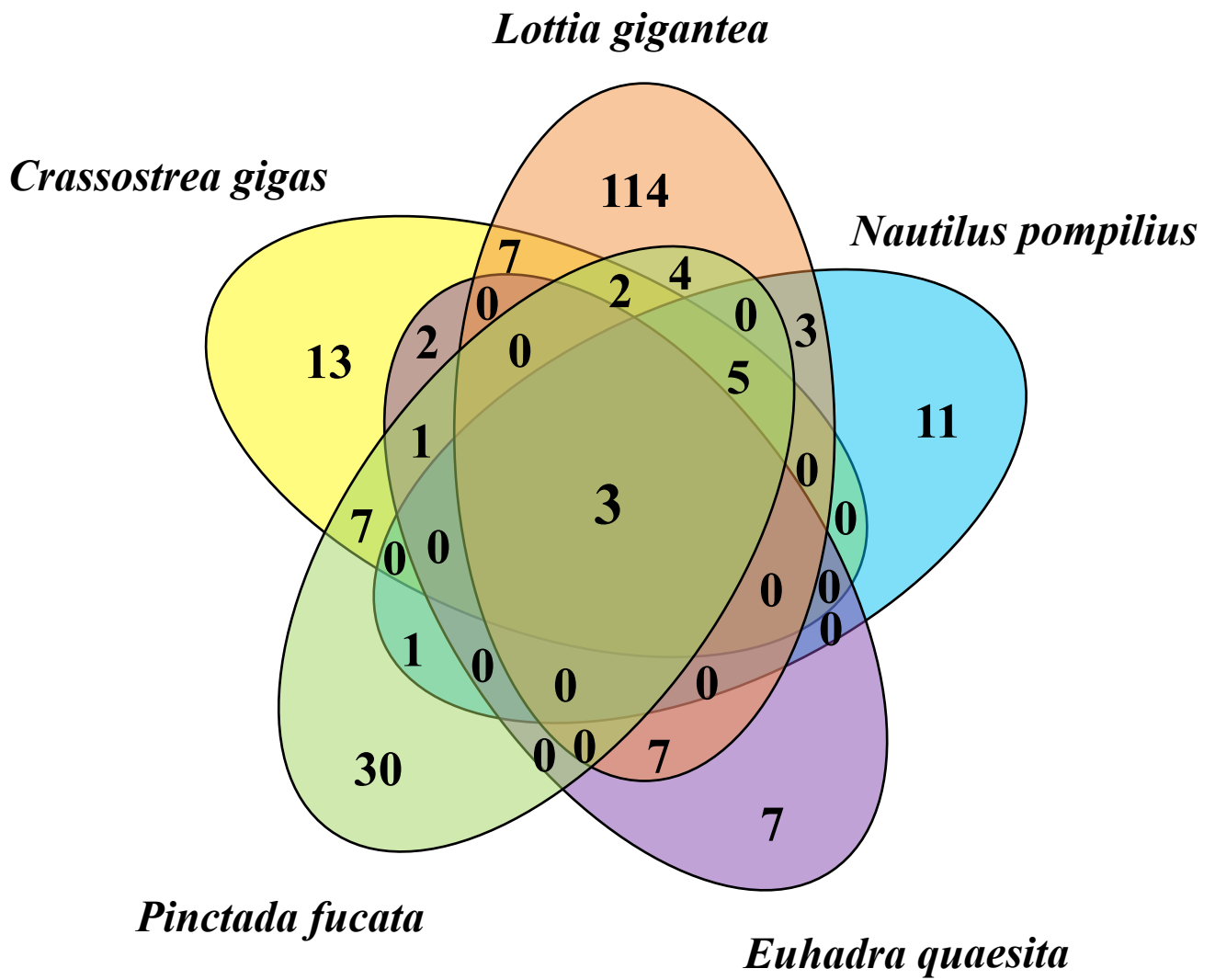


Fig. 3

C

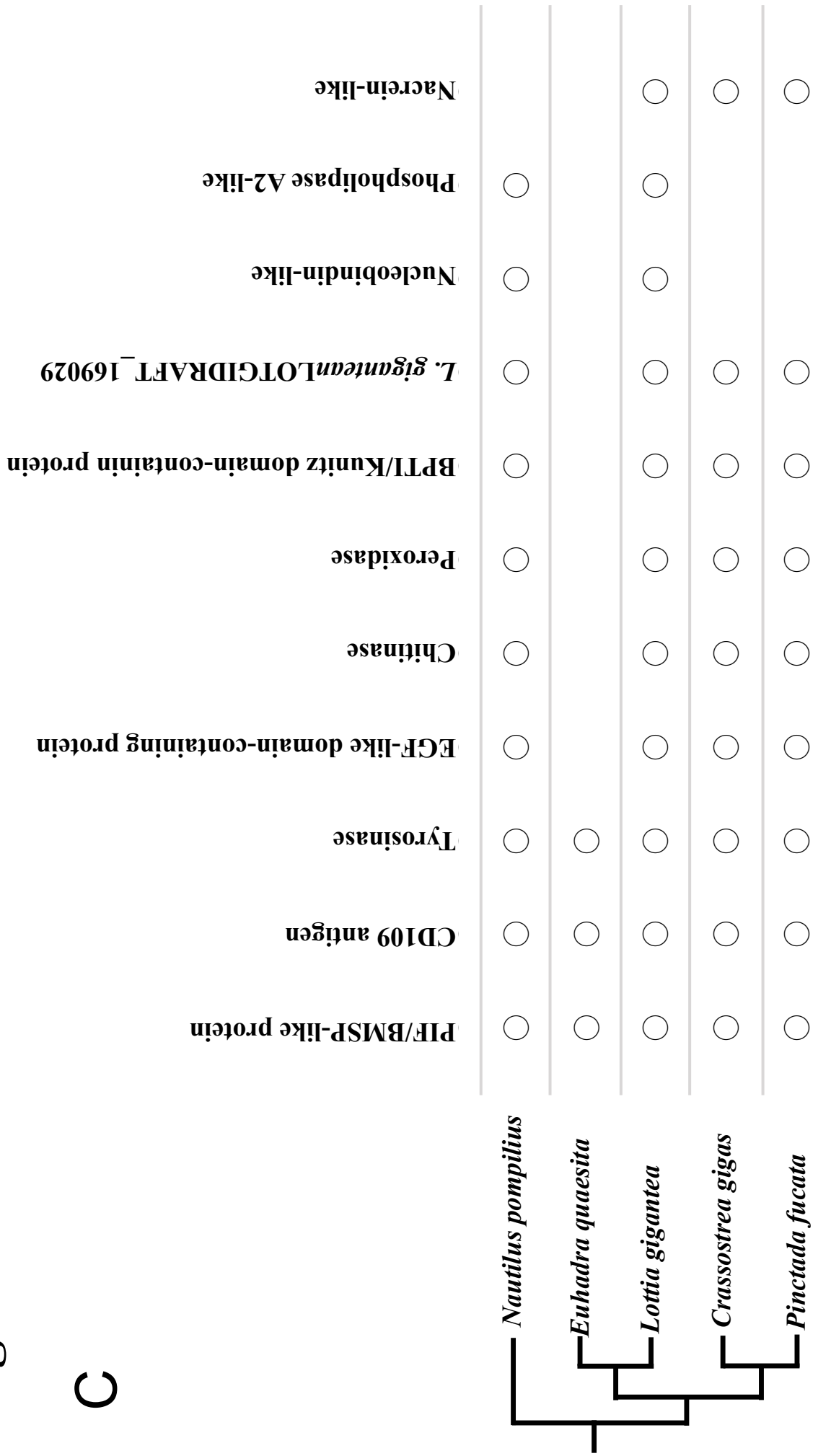


Fig. 4

A

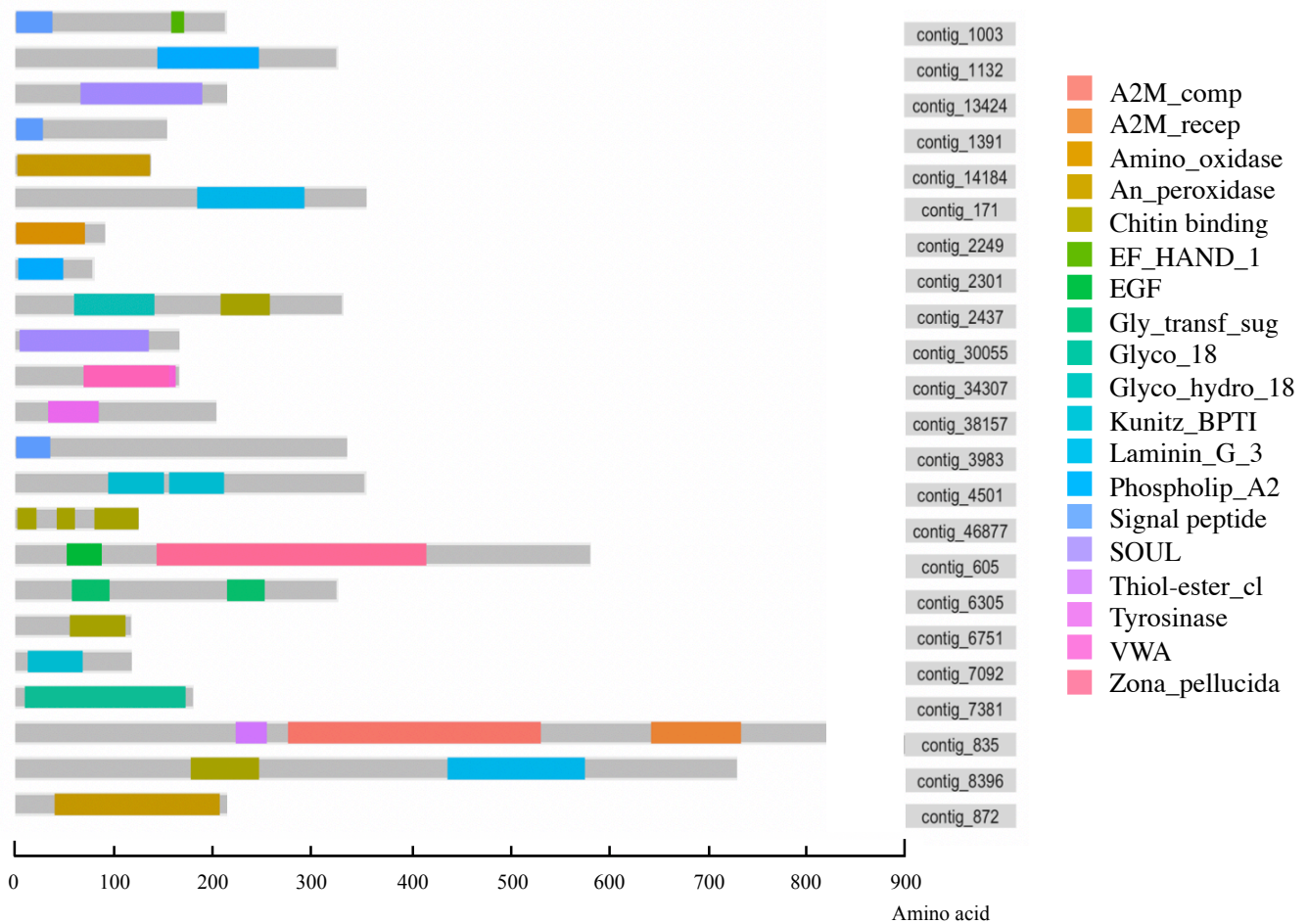


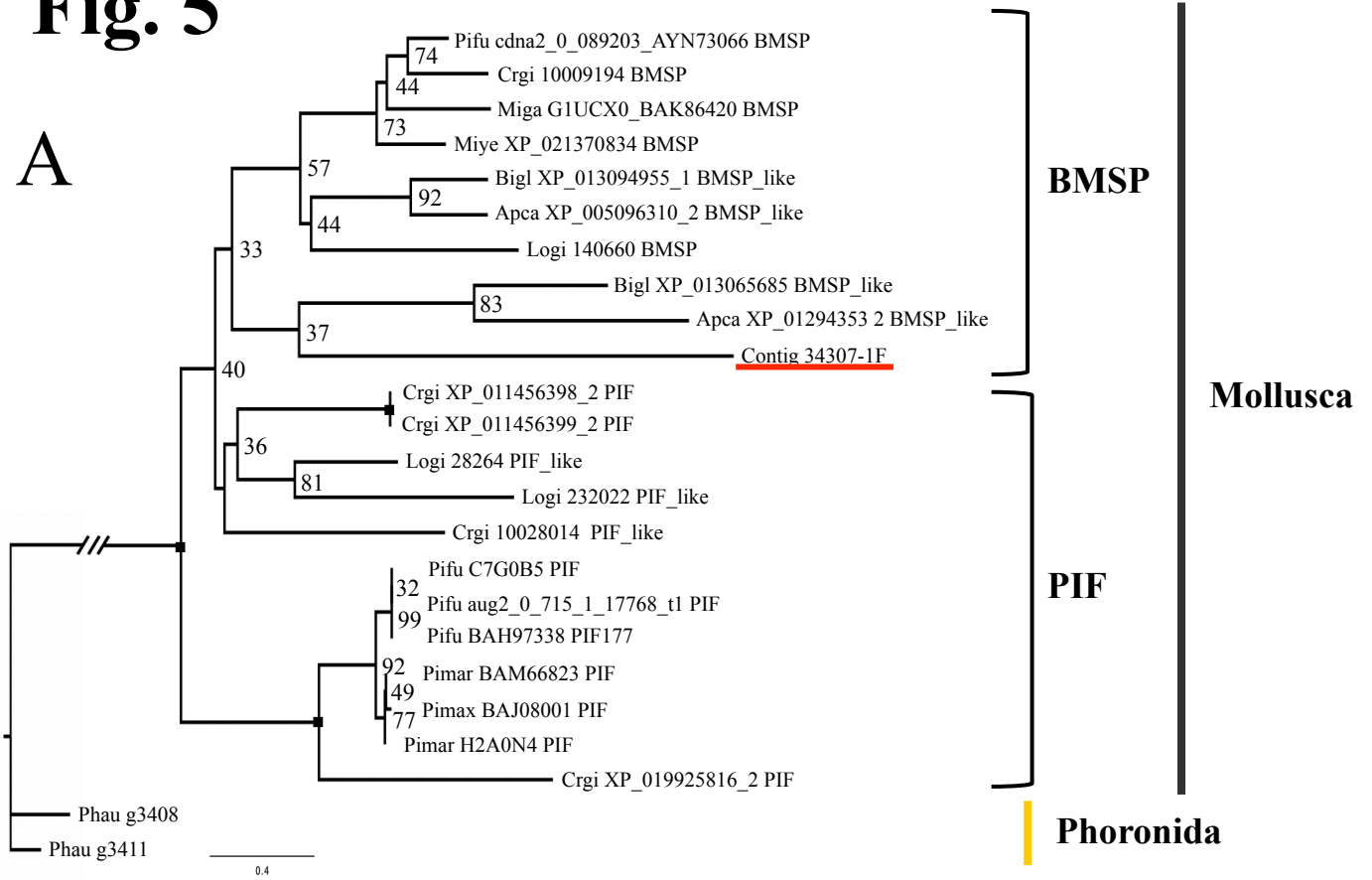
Fig. 4

B

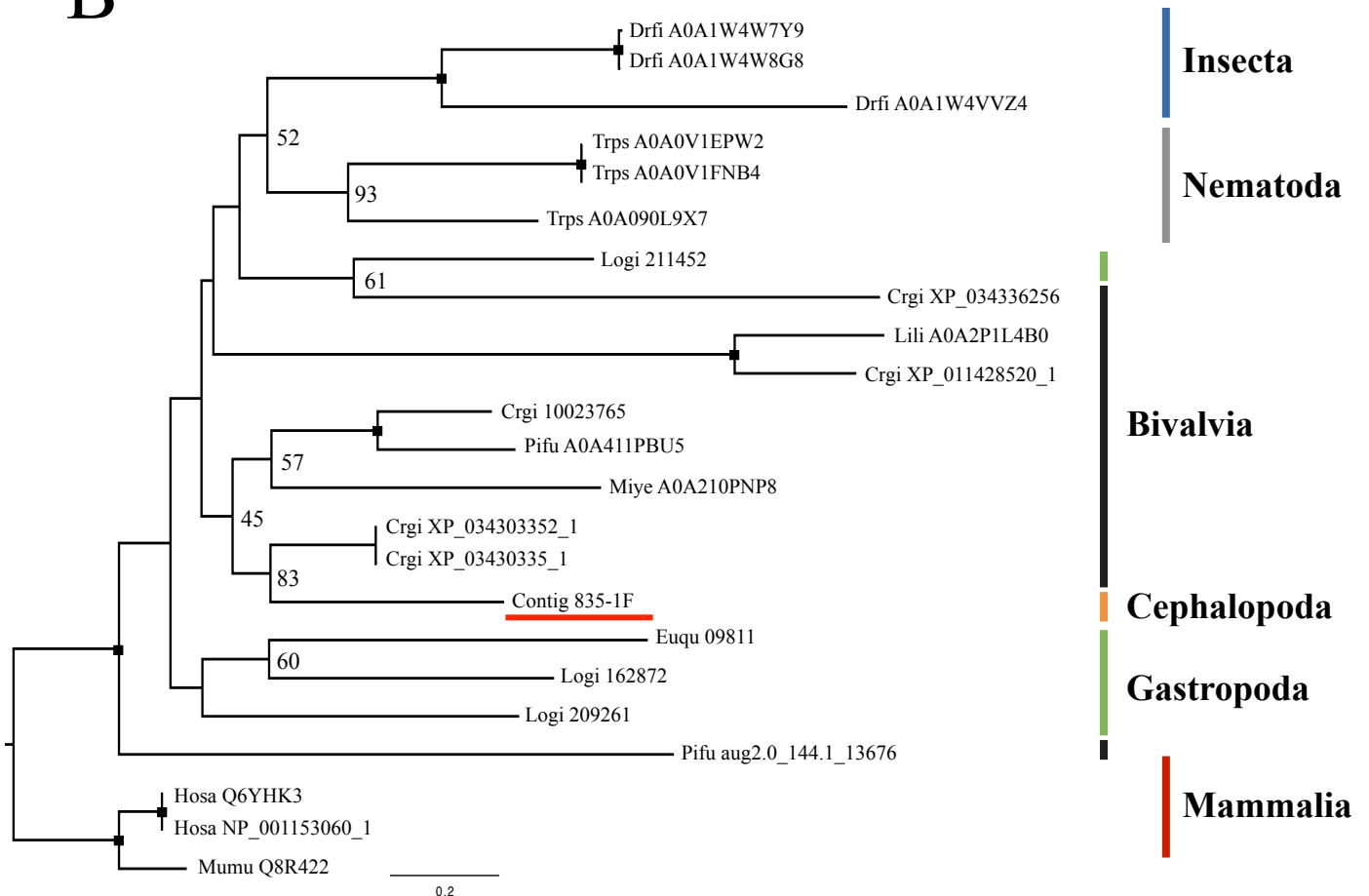


Fig. 5

A



B



C

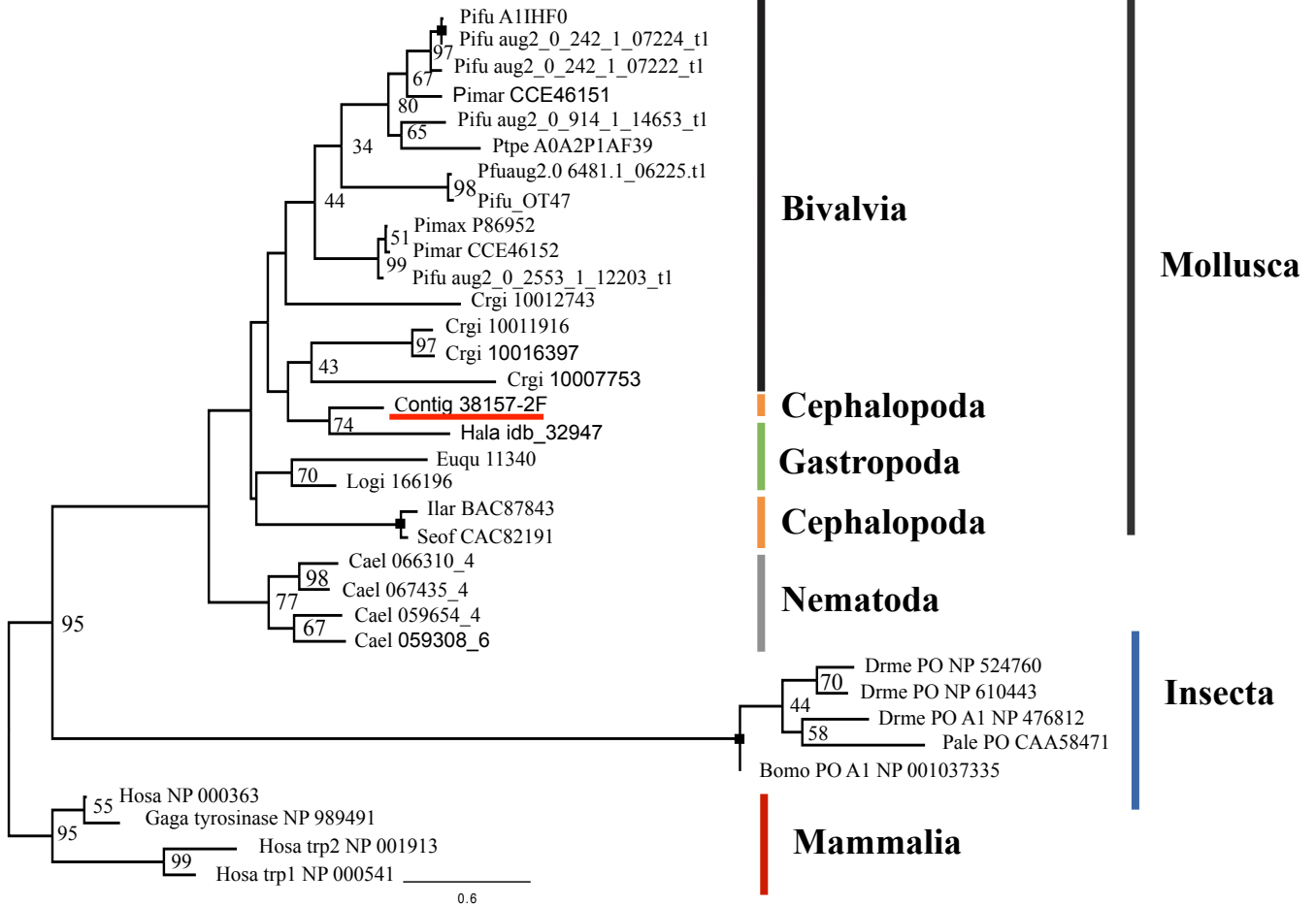


Fig. 5

D

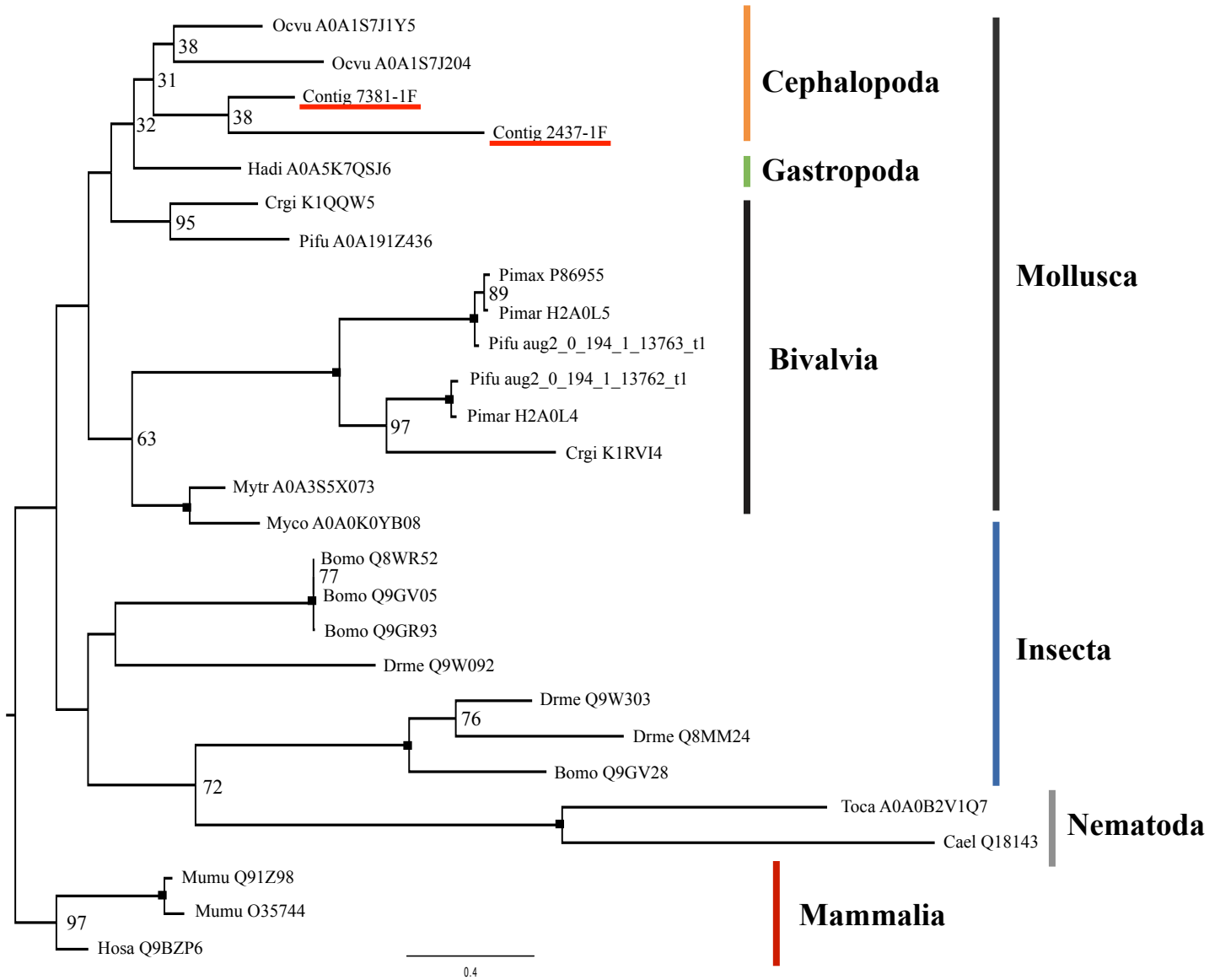


Fig. 5

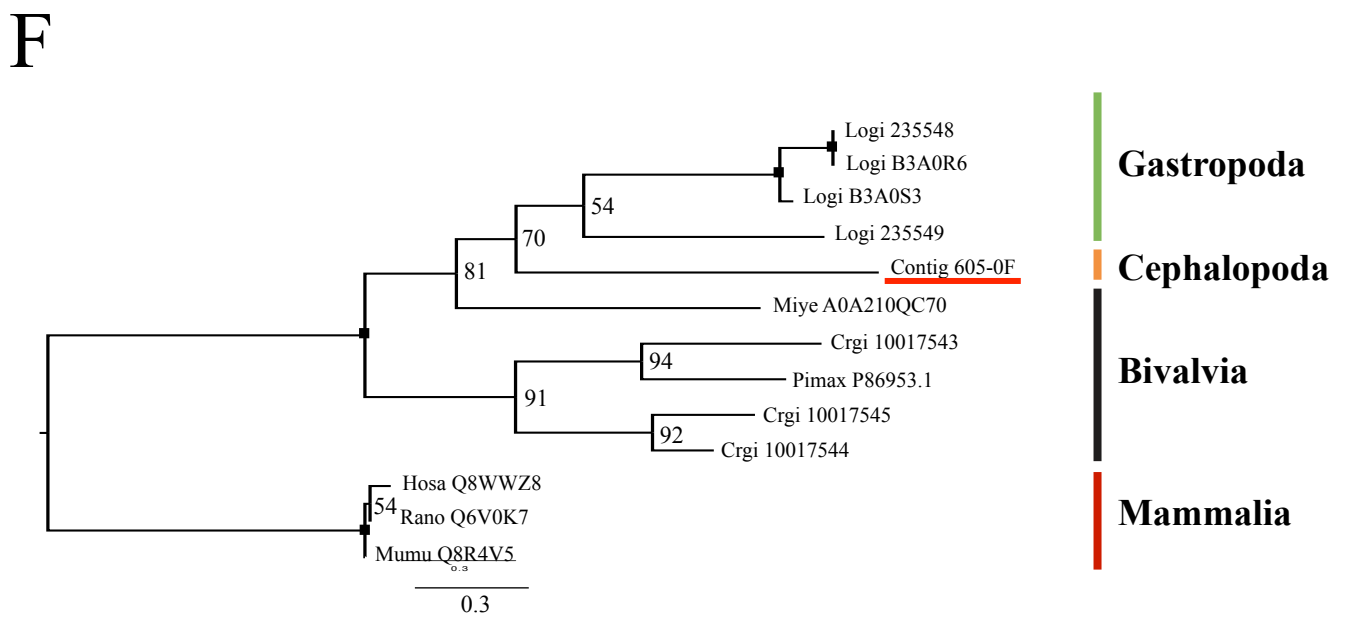
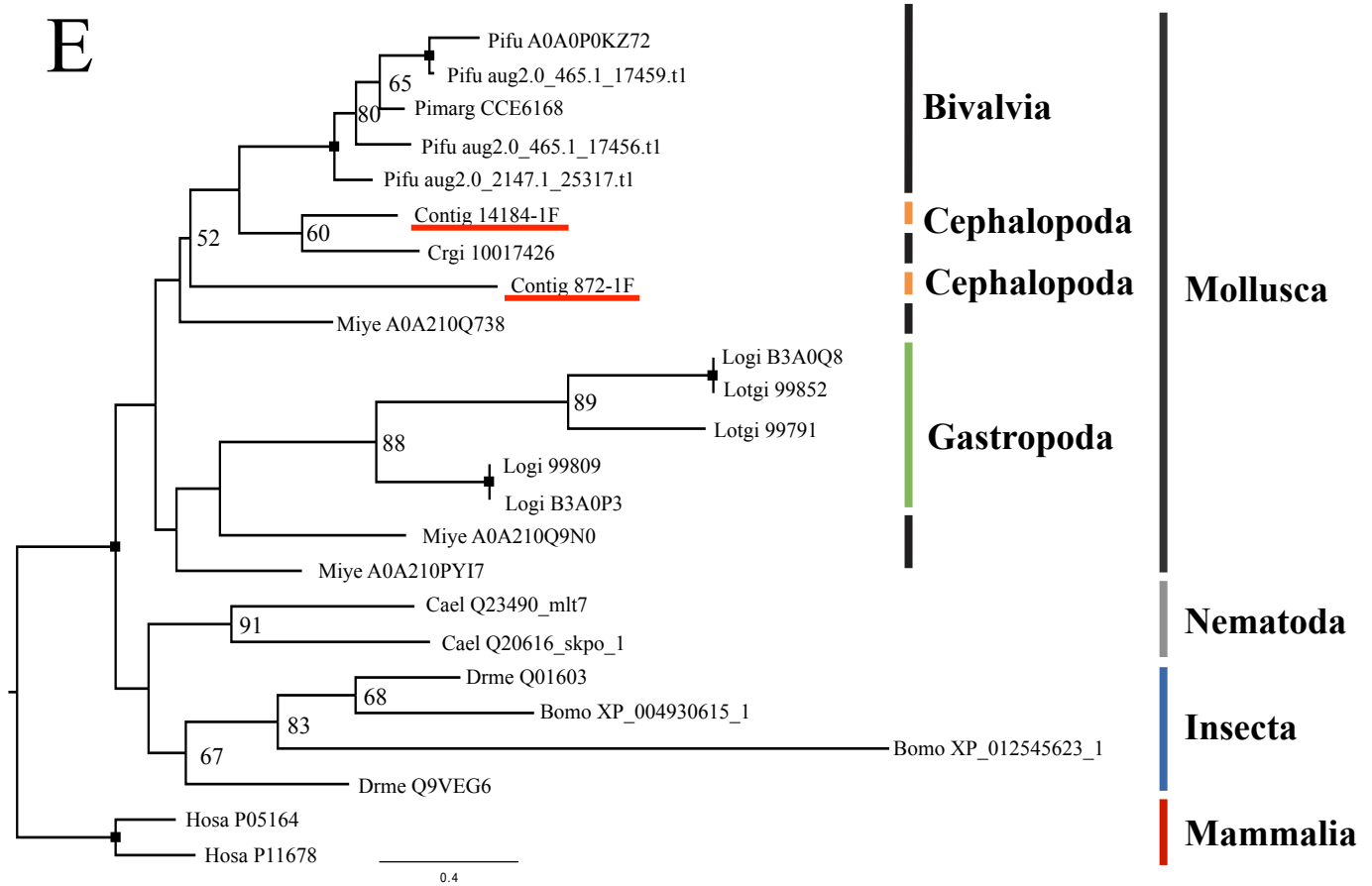


Table 1. The amount and quality of the data obtained from each tissue sample

Sample ID	individual#	tissue location	# reads	GC%
NBMantle	B	mantle - random	5,653,110	54.14%
NCMA	C	mantle - anterior	5,958,989	55.43%
NCML	C	mantle - left	6,434,608	56.06%
NCMR	C	mantle - right	5,965,524	55.49%
NCMP	C	mantle - posterior	5,299,856	54.85%
NDMP	D	mantle - posterior	5,976,728	54.11%
NDMA	D	mantle - anterior	6,475,168	55.57%

Table 2. The five most abundant transcripts with ORF (in the whole mantle sample) in the mantle tissue of *Nautilus pompilius*

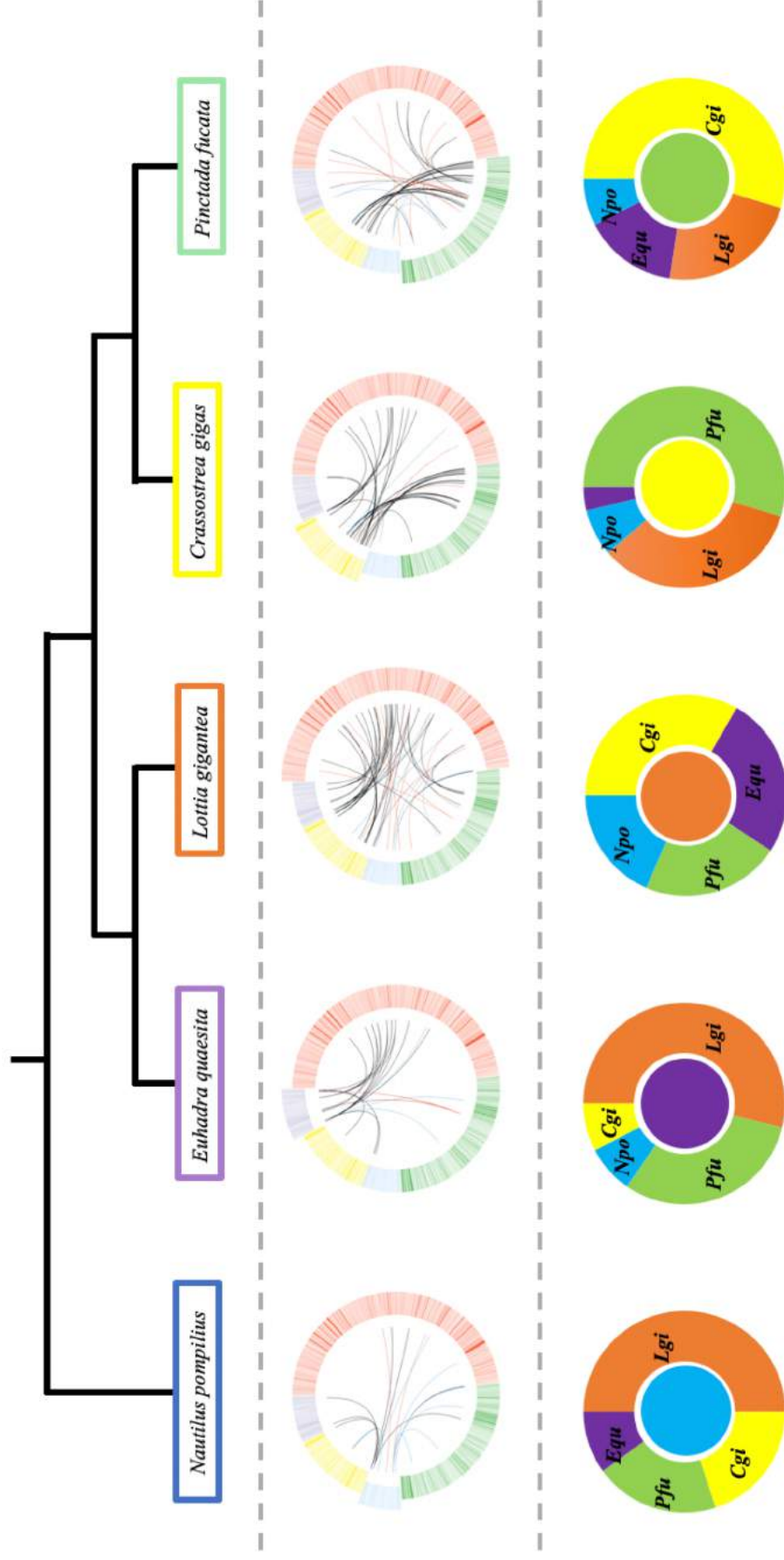
contig ID	FPKM	O. bimaculoides homolog	diamond e-value	hmm domain
contig_36199	3,124,349.10	Ocbimv22030012m.p	1.50E-30	No hit
contig_42552	1,328,691.40	None	-	No hit
contig_42075	841,970.80	None	-	No hit
contig_16011	460,159.50	Ocbimv22007851m.p	2.90E-42	No hit
contig_7243	323,500.20	None	-	No hit

Table 3. Annotation results of the 47 transcriptome contigs, which were identified as shell matrix protein-coding genes by proteome analysis

contig ID	e-value	BLAST against protein	e-value	Local BLASTp against known conchiferan SMPs	e-value
contig_130		None		None	
contig_145		None		None	
contig_171	1.92E-23	sushi-like protein [<i>Mytilus coruscus</i>]	3.00E-21	Shell matrix protein [<i>Mizuhopecten yessoensis</i>]	2.88E-19
contig_175		None		None	
contig_218		None		None	
contig_605	7.05E-95	PREDICTED: EGF-like domain-containing protein 2 isoform X3 [<i>Octopus bimaculoides</i>]	2.00E-107	Full=EGF-like domain-containing protein 2; AltName: Full=Uncharacterized shell protein 24; Short=LUSP-24; Flags: Precursor [<i>Lottia gigantea</i>]	4.32E-36
contig_737		None		None	
contig_749		None		None	
contig_790		None		None	
contig_835	2.57E-98	CD109 antigen-like isoform X1 [<i>Crassostrea gigas</i>]	0	None	
contig_872	1.17E-47	Chorion peroxidase-like [<i>Octopus vulgaris</i>]	3.00E-45	Chorion peroxidase [<i>Crassostrea gigas</i>]	6.55E-35
contig_1003		protein PFC0760c-like [<i>Octopus vulgaris</i>]	1.00E-03	None	
contig_1132	3.83E-19	phospholipase A2-like [<i>Centruroides sculpturatus</i>]	1.00E-39	None	
contig_1391		Ahypothetical protein KP79_PYT17609 [<i>Mizuhopecten yessoensis</i>]	6.00E-10	None	
contig_1429		None		None	
contig_2249		aplysianin-A-like [<i>Crassostrea virginica</i>]	9.00E-06	None	
contig_2301		hypothetical protein LOTGIDRAFT_176428 [<i>Lottia gigantea</i>]	3.00E-08	None	
contig_2437	3.85E-58	Chitinase [<i>Sepia esculenta</i>]	2.00E-42	chitinase-3 [<i>Hyriopsis cumingii</i>]	1.16E-37
contig_3214		hypothetical protein LOTGIDRAFT_236297 [<i>Lottia gigantea</i>]	1.00E-04	None	
contig_3983		None		None	
contig_4501	7.33E-15	papilin-like [<i>Lingula anatina</i>]	2.00E-37	RecName: Full=BPT1/Kunitz domain-containing protein [<i>Haliotis asinina</i>]	1.17E-24
contig_6305	1.38E-11	uncharacterized protein LOC112560033 isoform X3 [<i>Pomacea canaliculata</i>]	2.00E-24	None	
contig_6751	9.10E-16	BMSP [<i>Mytilus galloprovincialis</i>]	3.00E-19	BMSP [<i>Mytilus galloprovincialis</i>]	5.83E-25
contig_7092		collagen alpha-3(VI) chain isoform X2 [<i>Cricetulus griseus</i>]	6.00E-08	nacre serine protease inhibitor 5 [<i>Pinctada margaritifera</i>]	8.18E-54
contig_7381	4.32E-55	hypothetical protein OCBIM_22014960mg [<i>Octopus bimaculoides</i>]	3.00E-51	Chit3 protein [<i>Crassostrea gigas</i>]	8.18E-54
contig_8396	8.11E-27	Sushi-like protein [<i>Mytilus coruscus</i>]	6.00E-56	Shell matrix protein, partial [<i>Bathymodiolus platifrons</i>]	5.21E-52
contig_8398		None		None	
contig_11910	1.10E-12	PREDICTED: nucleobindin-1-like, partial [<i>Paralichthys olivaceus</i>]	2.00E-07	None	
contig_13424		heme-binding protein 2-like [<i>Limulus polyphemus</i>]	3.00E-08	None	
contig_14184	4.92E-44	Peroxidase-like protein [<i>Mizuhopecten yessoensis</i>]	9.00E-42	Chorion peroxidase [<i>Crassostrea gigas</i>]	5.56E-44
contig_14880		None		None	
contig_16223		None		None	
contig_17506		Protein PIF [<i>Mizuhopecten yessoensis</i>]	1.00E-02	BMSP-like protein [<i>Lottia gigantea</i>]	5.85E-08
contig_21095		None		None	
contig_21964		None		None	
contig_23085		None		None	
contig_25822		hypothetical protein KP79_PYT14004 [<i>Mizuhopecten yessoensis</i>]	9.00E-08	None	
contig_30055	4.35E-22	uncharacterized protein LOC106876168 [<i>Octopus bimaculoides</i>]	3.00E-18	None	
contig_30170	9.78E-16	mucin-5AC-like isoform X2 [<i>Pomacea canaliculata</i>]	4.00E-15	None	
contig_30322		None		None	
contig_33774		None		None	
contig_34307	4.58E-15	collagen-like protein-1, partial [<i>Mytilus coruscus</i>]	3.00E-13	BMSP [<i>Mytilus galloprovincialis</i>]	4.48E-16
contig_35294		None		None	
contig_38157	6.29E-81	tyrosinase-like protein [<i>Octopus vulgaris</i>]	3.00E-77	None	
contig_38801		None		None	
contig_46079		None		None	
contig_46877		hypothetical protein LOTGIDRAFT_169029 [<i>Lottia gigantea</i>]	3.00E-03	None	

Supplementary Fig. 1

E-value
 $1e-5 >$
 $50\% \leq$



Supplementary Table 1. Comparison of Shell Matrix Proteins of four Conchiforms under "Setting 1". Setting 1 was set the threshold of e50% sequence homology, and e-value of e-5

<i>Nautilus pompilius</i>		<i>Lottia gigantea</i>		<i>Euhadra quaesita</i>		<i>Euhadra quaesita</i>		<i>Pinctada fucata</i>					
contig_14184	Peroxidase-like protein [Mizuhopecten yessoensis]	Lotg1199791	Uncharacterized protein; domain: An_peroxidase Peroxidase_3						Peroxidase				
contig_14184	Peroxidase-like protein [Mizuhopecten yessoensis]	Lotg1199809	Uncharacterized protein; domain: An_peroxidase Peroxidase_3										
contig_14184	Peroxidase-like protein [Mizuhopecten yessoensis]	Lotg1199852	Uncharacterized protein; domain: An_peroxidase Peroxidase_3										
contig_30055	uncharacterized protein LOC106876168 [Octopus bimaculoides]	Lotg11205030	Uncharacterized protein; domain: SOUL						SOUL containing protein				
contig_605	Full-EGF-like domain-containing protein 2	Lotg11235548	Similar to gigasin-2 1; domains: EGF_ZP_2	CGI_10017543	Gigasins-2		pfu_aug2.0_2116.1_21941.11	EGF-like domain-containing protein 1 (Fragment)					
				CGI_10017544	EGF-like domain-containing protein 2		pfu_aug2.0_2116.1_21942.11	EGF-like domain-containing protein 2	EGF-ZP domain containing protein				
				CGI_10017545	EGF-like domain-containing protein 2		pfu_aug2.0_2116.1_21943.11	EGF-like domain-containing protein 2					
							pfu_aug2.0_3578.1_29138.11	EGF-like domain-containing protein 1 (Fragment)					
						pfu_aug2.0_838.1_27830.11	EGF-like domain-containing protein 2						
contig_835	CD109 antigen-like isoform X1 [Crassostrea gigas]	Lotg11162872	Similar to thioester-containing protein; domains: a2-macroglobulin	CGI_10023785	CD109 antigen	Equ09811	Thioester-containing protein		CD109 antigen				
				Lotg11211452	Similar thioester-containing protein; a2-macroglobulin family								
contig_6396	bush-like protein [Mytilus conus]	Lotg11228264	Similar to PHS7/BMSP 1; domains: vWA, chitin-binding	CGI_10012353	Protein PIF	Equ10634	Uncharacterized protein	pfu_aug2.0_7063.1_12916.11	Shell matrix protein (Fragment)				
contig_171	uncharacterized protein LOC110461617 [Mizuhopecten yessoensis]	Lotg11232022	Similar to PHS7/BMSP 1; domains: vWA, chitin-binding					pfu_aug2.0_160.1_00336.11	Uncharacterized shell protein 26 (Fragment)				
								Lotg11231395	Uncharacterized protein; domains: 2 x chitin-binding pentrophin-A; some similarity to PIF/BMSP 1			pfu_aug2.0_747.1_24369.11	-
								Lotg11237510	Similar to chitin-binding protein P86860 1			pfu_aug2.0_929.1_31288.11	Protein PIF
								pfu_aug2.0_715.1_17788.11	Protein PIF				

Supplementary Table 3. The domains of *Nautilus pompilius* as predicted by SMART, PROSITE NCBI and InterProScan

ID	Domain				Domain Conclusion
	SMART	PROSITE	NCBI	InterProScan	
contig_11910			peroxinectin_like		
contig_14184	Pfam:An_peroxidase	PEROXIDASE_3	An_peroxidase PLN02283		An_peroxidase
contig_171			Laminin_G_3		Laminin_G_3
contig_17506			Amino_oxidase		Amino_oxidase
contig_2249			Phospholip_A2_3		Phospholipase A2
contig_2301			GH18_chitolectin_chit otriosidase		
contig_2437	Pfam:Glyco_hydro_18 ChtBD2	CHIT_BIND_II	Glyco_18 CBM_14 ChtBD2 Glyco_hydro_18	Glycoside hydrolase family 18, catalytic domain Chitin binding domain	Glyco_hydro_18 Chitin binding
contig_30055	Pfam:SOUL		SOUL		SOUL
contig_30322			VWA		
contig_34307	Pfam:VWA_2 Pfam:VWA	VWFA	vWFA_subfamily_ECM ChiD	von Willebrand factor, type A	von Willebrand factor, type A
contig_38157	Pfam:Tyrosinase signal peptide		Tyrosinase		Tyrosinase
contig_4501	KU	BPTL_KUNITZ_1 BPTL_KUNITZ_2	Kunitz_BPTI KU	Pancreatic trypsin inhibitor Kunitz domain	signal peptide Kunitz
contig_46877	transmembrane region Pfam:CBM_14	CHIT_BIND_II			Chitin binding
contig_605	transmembrane region EGF ZP	EGF_3 ZP_2 EGF_1	ZP Zona_pellucida		Zona_pellucida EGF
contig_6751	ChtBD2	CHIT_BIND_II	ChtBD2 CBM_14	Chitin binding domain	Chitin binding
contig_7092	KU	BPTL_KUNITZ_2	KU Kunitz_BPTI GH18_chitolectin_chit otriosidase	Pancreatic trypsin inhibitor Kunitz domain	Kunitz
contig_7381	Glyco_18		Glyco_18 Glyco_hydro_18 ChiA	Glycoside hydrolase family 18, catalytic domain Chitinase II	Glyco_18
contig_835	Thiol-ester_cl Pfam:A2M_comp A2M_recep		A2M_2 A2M_comp A2M_recep YfaS		A2M_comp A2M_recep Thiol-ester_cl
contig_8396	ChtBD2	CHIT_BIND_II		Chitin binding domain	Chitin binding
contig_872	Pfam:An_peroxidase	PEROXIDASE_3	peroxinectin_like An_peroxidase PLN02283		An_peroxidase

Supplementary Table 4. The domain of 4 species (*Pinctada fucata*, *Lotia gigantea*, *Euhadra quaesta*, and *Crasostrea gigas*) as predicted by SMART.

<i>Pinctada fucata</i>		<i>Lotia gigantea</i>		<i>Euhadra quaesta</i>		<i>Crasostrea gigas</i>	
ID	Domain	ID	Domain	ID	Domain	ID	Domain
pfu_sug2.0.1101.1_04821.11	KU	Lotg1101611	Sod_Cu	Equ02505	ACTIN	CGL_10003000	C1Q
pfu_sug2.0.1101.1_04822.11	KU	Lotg1113221	Antistatin	Equ02555	ACTIN	CGL_10004086	WVA
pfu_sug2.0.1101.1_04823.11	Signal peptide	Lotg1121860	EF-hand_7	Equ04504	ACTIN	CGL_10004228	Signal peptide
pfu_sug2.0.1101.1_04825.11	KU	Lotg1124263	Cu-oxidase Cu-oxidase_2 Cu-oxidase_3	Equ09762	ACTIN	CGL_10005425	Beta-lactamase Signal peptide
pfu_sug2.0.1225.1_18190.11	Signal peptide SCOP d1cxp.1	Lotg1126004	UBO	Equ09811	ASM_comp ASM_recep	CGL_10005749	Signal peptide
pfu_sug2.0.126.1_20287.11	Galactosyl_T	Lotg1132911	KU	Equ10634	Chitin binding	CGL_10007021	SSF WVC
pfu_sug2.0.1358.1_28227.11	Cu2_monooxygen Cu2_monoox_C	Lotg1138864	DnaJ DnaJ_C	Equ11340	Tyrosinase	CGL_10007753	Tyrosinase
pfu_sug2.0.1414.1_16516.11	An peroxidase Signal peptide	Lotg1140660	VWA	Equ12964	C1Q	CGL_10007857	CHB_HEX Glyco_hydro_20b Glyco_hydro_20 Cu-oxidase Cu-oxidase_2 Cu-oxidase_3
pfu_sug2.0.144.1_13678.11	AS2M_N AS2M AS2M_recep AS2M_comp Thiol_ester_cl	Lotg1155090	DnaJ Tetrapeptide repeat- containing CLECT LDLa	Equ14133	VWA	CGL_10008969	SCOP d1repw1
pfu_sug2.0.160.1_00336.11	Signal peptide	Lotg1156525	CUB CCP EGF_CA RPT_1	Equ15522-15523	CCP Signal peptide	CGL_10010359	GTP_EFTU
pfu_sug2.0.160.1_00336.11	Signal peptide	Lotg1159173	Phospholip_A2_3	Equ20990	GTP_EFTU	CGL_10010526	Signal peptide
pfu_sug2.0.1638.1_28429.11	KU	Lotg1160173	Chitin binding Signal peptide	Equ21047	Porin_3	CGL_10011916	Tyrosinase
pfu_sug2.0.1638.1_28435.11	KU	Lotg1162671	UBO	Equ21150		CGL_10012348	IG IGc2 Chitin binding
pfu_sug2.0.164.1_13717.11	Tryp_SPC	Lotg1162872	AS2M_N AS2M_N_2 AS2M Thiol_ester_cl AS2M_comp AS2M_recep	Equ21247	CCP Signal peptide	CGL_10012352	IGc2 Chitin binding
pfu_sug2.0.1919.1_31963.11	C1Q Signal peptide	Lotg1163637	SCOP d1gw5a	Equ21466	Polysacc_deac_1	CGL_10012353	EGF Chitin binding GTP_EFTU
pfu_sug2.0.194.1_13762.11	Glyco_18	Lotg1166196	Tyrosinase Signal peptide	Equ22322	C1Q	CGL_10012474	GTP_EFTU_D2 GTP_EFTU_D3
pfu_sug2.0.194.1_13763.11	Glyco_18 Chitin binding Signal peptide	Lotg1168464	Porin_3	Equ22329	C1Q	CGL_10012743	Tyrosinase
pfu_sug2.0.210.1_00425.11	Sulfotransfer_2 Chitin binding	Lotg1171918	Antistatin WR1 Signal peptide	Equ22616	UBO Ribosomal L40e	CGL_10013347	AAA
pfu_sug2.0.216.1_21941.11	ZP EGF	Lotg1173138	Chitin binding	Equ23617-24364	MA	CGL_10013462	LPMO_10 Signal peptide Carb_anhydrase
pfu_sug2.0.216.1_21942.11	ZP EGF Signal peptide	Lotg1175997	H4 H2B	Equ28417		CGL_10014170	Globin
pfu_sug2.0.216.1_21943.11	ZP	Lotg1176428	Phospholip_A2_3	Equ32891	UBO	CGL_10015381	Tryp_SPC Signal peptide KU
pfu_sug2.0.214.1_13802.11	Carb_anhydrase	Lotg1176483	VWC	Equ53877	H4	CGL_10015567	Tyrosinase AT_hook PHD RING PDB 2YUKA Glyco_hydro_9
pfu_sug2.0.217.1_25317.11	An peroxidase Signal peptide	Lotg1176498	H3			CGL_10016397	
pfu_sug2.0.219.1_30448.11	VWA CCP Chitin binding Signal peptide	Lotg1181237	Polysacc_deac_1 Signal peptide			CGL_10016430	
pfu_sug2.0.242.1_07222.11	Tyrosinase Signal peptide	Lotg1193218	ACTIN			CGL_10016964	FN3 Signal peptide
pfu_sug2.0.242.1_07224.11	Tyrosinase Signal peptide	Lotg1201804	WAP Antistatin Lustrin_cysteine WR1			CGL_10016965	FN3
pfu_sug2.0.244.1_12165.11	PDB 2C1WC SD	Lotg1201876	ATP-synt_ab_N AAA			CGL_10016966	FN3
pfu_sug2.0.255.1_12203.11	Tyrosinase	Lotg1202971	ACTIN			CGL_10017087	Chitin binding
pfu_sug2.0.261.1_12244.11	An peroxidase VWD	Lotg1203293	ADF			CGL_10017428	An_peroxidase ZP
pfu_sug2.0.269.1_30539.11	DUF1943 LPD_N	Lotg1205030	SOUL Signal peptide			CGL_10017543	EGF Signal peptide ZP
pfu_sug2.0.275.1_17228.11	KU	Lotg1205401	Carb_anhydrase			CGL_10017544	EGF Signal peptide ZP
pfu_sug2.0.290.1_25577.11	Antistatin Signal peptide	Lotg1205506	ACTIN			CGL_10017545	EGF Signal peptide
pfu_sug2.0.290.1_25578.11	KU Antistatin	Lotg1206617	ATP-synt_ab_N ATP-synt_ab_C Glyco_18 Signal peptide AS2M_N AS2M_N_2 AS2M			CGL_10018176	LPMO_10 Signal peptide
pfu_sug2.0.292.1_09016.11	ADF	Lotg1209107	Sod_Cu Signal peptide			CGL_10018834	Sod_Cu Signal peptide
pfu_sug2.0.297.1_23818.11	Chitin binding Signal peptide	Lotg1209281	AS2M Thiol_ester_cl AS2M_comp AS2M_recep AS2M			CGL_10020756	KU
pfu_sug2.0.3.1_10035.11	LPMO_10 Signal peptide	Lotg1211452	Thiol_ester_cl AS2M_comp AS2M_recep Pro_isomerase Signal peptide			CGL_10021817	LPD_N DUF1943 VWD Signal peptide
pfu_sug2.0.3578.1_29138.11	ZP EGF	Lotg1212757	Pro_isomerase Signal peptide			CGL_10022480	SCP
pfu_sug2.0.38.1_30047.11	LPMO_10	Lotg1215510	ACTIN			CGL_10023765	AS2M Thiol_ester_cl AS2M_comp AS2M_recep
pfu_sug2.0.3932.1_09248.11	VWA Chitin binding Signal peptide	Lotg1216792	XendoU			CGL_10023767	AS2M_N AS2M_N_2
pfu_sug2.0.429.1_30750.11	FN3	Lotg1222979	Pro_isomerase Signal peptide			CGL_10023851	Pro_isomerase
pfu_sug2.0.429.1_30751.11	FN3	Lotg1226726	LPMO_10 Signal peptide			CGL_10024501	ATP-synt_ab_N ATP-synt_ab ATP-synt_ab_C
pfu_sug2.0.429.1_30752.11	FN3 SCOP d1tq3a1 Signal peptide	Lotg1228264	VWA Chitin binding Signal peptide AS2M_N AS2M_N_2 Signal peptide			CGL_10026605	Glyco_18 Chitin binding
pfu_sug2.0.465.1_17456.11	An peroxidase	Lotg1229818	AS2M_N AS2M_N_2 Signal peptide			CGL_10028014	VWA Chitin binding Signal peptide
pfu_sug2.0.465.1_17459.11	An peroxidase	Lotg1230854	VWC			CGL_10028296	WR1 WVC
pfu_sug2.0.470.1_00785.11	C1Q Signal peptide	Lotg1231395	SCOP d1c4ra Chitin binding Signal peptide			CGL_10028414	VWC
pfu_sug2.0.490.1_00814.11	DnaJ Signal peptide CLECT	Lotg1231869	Chitin binding			CGL_10028495	Carb_anhydrase Signal peptide
pfu_sug2.0.495.1_17489.11	Homr1 GAIN GPS	Lotg1232022	VWA Chitin binding				
pfu_sug2.0.53.1_10184.11	Laminin_G_3 Chitin binding	Lotg1232718	EGF Signal peptide				
pfu_sug2.0.5814.1_16145.11	Signal peptide CHB_HEX	Lotg1233138	UBO				
pfu_sug2.0.6.1_20028.11	Glyco_hydro_20b Glyco_hydro_20	Lotg1233199	SCP Signal peptide				
pfu_sug2.0.608.1_27581.11	Amino_oxidase	Lotg1233200	SCP Signal peptide				
pfu_sug2.0.6481.1_06225.11	NAD_binding_9 Tyrosinase Signal peptide	Lotg1233201	SCP Signal peptide				
pfu_sug2.0.701.1_04487.12	SH_KT SCP	Lotg1234386	Signal peptide				
pfu_sug2.0.7063.1_12916.11	Laminin_G_3 Chitin binding VWA	Lotg1234387					
pfu_sug2.0.715.1_17768.11	Chitin binding Signal peptide	Lotg1234405	Chitin binding Signal peptide				
pfu_sug2.0.729.1_31106.11	KU	Lotg1234561	UBO EGF ZP				
pfu_sug2.0.747.1_24365.11	Chitin binding	Lotg1235548	Signal peptide EGF ZP CLECT Sh_KT				
pfu_sug2.0.747.1_24368.11	Chitin binding	Lotg1235549					
pfu_sug2.0.747.1_24369.11	SCOP d1c4ra EGF Chitin binding ZP	Lotg1236690	Signal peptide				
pfu_sug2.0.838.1_27830.11	Signal peptide	Lotg1237510	Laminin_G_3 Carb_anhydrase WAP				
pfu_sug2.0.853.1_11239.11	Signal peptide	Lotg1238082	WR1 Antistatin Signal peptide				
pfu_sug2.0.862.1_07957.11	WR1	Lotg1239125	Carb_anhydrase Signal peptide				
pfu_sug2.0.8781.1_06362.11	Beta-lactamase	Lotg1239188	Chitin binding Signal peptide				
pfu_sug2.0.914.1_14653.11	Tyrosinase	Lotg1239574	Chitin binding Signal peptide				
pfu_sug2.0.914.1_14654.11	Tyrosinase	Lotg1239701	An_peroxidase				
pfu_sug2.0.929.1_31288.11	Chitin binding Th4	Lotg1239809	An_peroxidase				
pfu_sug2.0.94.1_13574.11	ETF_QD FAD_binding_2 Chitin binding VWA	Lotg1239852	An_peroxidase				
pfu_cdn2.0_089203	Chitin binding Signal peptide						

Supplementary Table 5. Comparison of the conserved domains of 5 species (*Nautilus pompilius*, *Pinctada fucata*, *Lottia gigantea*, *Euhadra quaesita*, and *Crassostrea gigas*) in Conchifera

<i>N. po</i>	<i>P. fu</i>	<i>L. gi</i>	<i>E. qu</i>	<i>C. gi</i>
A2M_comp	A2M_comp	A2M_comp	A2M_comp	A2M_comp
A2M_recep	A2M_recep	A2M_recep	A2M_recep	A2M_recep
Chitin binding signal peptide	Chitin binding signal peptide	Chitin binding signal peptide	Chitin binding signal peptide	Chitin binding signal peptide
Tyrosinase	Tyrosinase	Tyrosinase	Tyrosinase	Tyrosinase
VWA	VWA	VWA	VWA	VWA
ZP	ZP	ZP		ZP
KU	KU	KU		KU
EGF	EGF	EGF		EGF
An_peroxidase	An_peroxidase	An_peroxidase		An_peroxidase
Glyco_18	Glyco_18	Glyco_18		Glyco_18
Thiol-ester_cl	Thiol ester cl	Thiol-ester_cl		Thiol-ester_cl
Laminin_G_3	Laminin_G_3	Laminin_G_3		
Amino_oxidase	Amino_oxidase			
Phospholip_A2_3		Phospholip_A2_3		
SOUL		SOUL		
	CCP	CCP	CCP	
	A2M	A2M		A2M
	A2M_N	A2M_N		A2M_N
	Carb_anhydrase	Carb_anhydrase		Carb_anhydrase
	LPMO_10	LPMO_10		LPMO_10
	SCP	SCP		SCP
	WR1	WR1		WR1
	C1Q		C1Q	C1Q
	ADF	ADF		
	Antistasin	Antistasin		
	CLECT	CLECT		
	DnaJ	DnaJ		
	DnaJ_C	DnaJ_C		
	H3	H3		
	Sh KT	Sh KT		
	Beta-lactamase			Beta-lactamase
	CHB_HEX			CHB_HEX
	DUF1943			DUF1943
	FN3			FN3
	Glyco_hydro_20			Glyco_hydro_20
	Glyco_hydro_20b			Glyco_hydro_20b
	LPD_N			LPD_N
	Tryp_SPc			Tryp_SPc
	VWD			VWD
		ACTIN	ACTIN	
		H4	H4	
		Polysacc_deac_1	Polysacc_deac_1	
		Porin_3	Porin_3	
		UBQ	UBQ	
		A2M_N_2		A2M_N_2
		AAA		AAA
		ATP-synt_ab		ATP-synt_ab
		ATP-synt_ab_C		ATP-synt_ab_C
		ATP-synt_ab_N		ATP-synt_ab_N
		Cu-oxidase		Cu-oxidase
		Cu-oxidase_2		Cu-oxidase_2
		Cu-oxidase_3		Cu-oxidase_3
		Pro_isomerase		Pro_isomerase
		Sod_Cu		Sod_Cu
		VWC		VWC
			GTP_EFTU	GTP_EFTU

Supplementary Table 6. The specific domains of 5 species (*Nautilus pompilius*, *Pinctada fucata*, *Lottia gigantea*, *Euhadra quaesita*, and *Crassostrea gigas*) in Conchifera

Npo	Pfu	Lgi	Equ	Cgi
Glyco_hydro_18	Cu2_monoox_C	CUB	MA	AT_hook
	7tm_2	EF-hand_7	Ribosomal L40e	Globin
	Cu2_monooxygen	EGF CA		Glyco_hydro_9
	ETF_QO	H2B		GTP_EFTU_D2
	FAD_binding_2	LDLa		GTP_EFTU_D3
	GAIN	Lustrin_cystein		IG
	Galactosyl_T	RPT 1		IGc2
	GPS	SCOP d1c4ra_		PDB 2YUK A
	HormR	SCOP d1gw5a		PHD
	NAD_binding_9	Tetratricopeptide repeat-containing domain		RING
	PDB 2C1W C			SCOP d1epwa1
	SCOP d1c4ra			SSF
	SCOP d1qg3a1			
	SCOP g1cxp.1			
	SO			
	Sulfotransfer_2			
	Thi4			